# Map of fluid flow in fractal porous medium into fractal continuum flow

Alexander S. Balankin and Benjamin Espinoza Elizarraraz
*Grupo "Mecánica Fractal," Instituto Politécnico Nacional, México, Distrito Federal, Mexico 07738*
(Received 7 March 2012; published 30 May 2012)

This paper is devoted to fractal continuum hydrodynamics and its application to model fluid flows in fractally permeable reservoirs. Hydrodynamics of fractal continuum flow is developed on the basis of a self-consistent model of fractal continuum employing vector local fractional differential operators allied with the Hausdorff derivative. The generalized forms of Green-Gauss and Kelvin-Stokes theorems for fractional calculus are proved. The Hausdorff material derivative is defined and the form of Reynolds transport theorem for fractal continuum flow is obtained. The fundamental conservation laws for a fractal continuum flow are established. The Stokes law and the analog of Darcy's law for fractal continuum flow are suggested. The pressure-transient equation accounting the fractal metric of fractal continuum flow is derived. The generalization of the pressure-transient equation accounting the fractal topology of fractal continuum flow is proposed. The mapping of fluid flow in a fractally permeable medium into a fractal continuum flow is discussed. It is stated that the spectral dimension of the fractal continuum flow $d_s$ is equal to its mass fractal dimension $D$, even when the spectral dimension of the fractally porous or fissured medium is less than $D$. A comparison of the fractal continuum flow approach with other models of fluid flow in fractally permeable media and the experimental field data for reservoir tests are provided.

DOI: 10.1103/PhysRevE.85.056314 PACS number(s): 47.53.+n, 47.56.+r, 47.10.ab

## I. INTRODUCTION

Fluid flow in permeable media plays an important role in a wide variety of environmental and technological processes [1]. Natural porous and/or fissured materials usually possess formidably complicated architecture characterized by statistical scale invariance over many length scales [2–4]. In this context, the fractal geometry offers helpful scaling concepts to quantify fluid transport in fractally permeable media. Consequently, different approaches have been addressed to the problems related to the fluid flow in fractal reservoirs (see Refs. [5–8] and references therein).

In a recent Rapid Communication [8] we have suggested that essentially discontinuous fractal flow $\Phi^D$ in a fractally permeable medium can be mapped to the fractal continuum flow $\Phi^3_D \subset E^3$, which is describable within a continuum framework (see Fig. 1). From this perspective, in Ref. [8] a self-consistent model of fractal continuum flow employing the local fractional differential operators was suggested, the fundamental conservation laws and the generalized Navier-Stokes equations for an anisotropic fractal continuum flow were derived, and some features of fractal continuum flow were discussed. It should be emphasized that the geometric framework of fractal continuum hydrodynamics is the three-dimensional Euclidean space with a fractal metric.

In this paper, the hydrodynamics continuum flow is advanced to account for the flow topology and employed to model fluid flow in a fractal porous (fissured) medium. The paper is organized as follows. In Sec. II the fractal properties of fractally permeable media are outlined. In Sec. III the concept of fractal continuum flow is generalized to account for nontrivial topology and dynamics of fractal continua ${}^{d_s}_{d_\ell}\Phi^3_D$. The vector local fractional differential operators allied with the Hausdorff derivative are developed. The generalized forms of Green-Gauss and Kelvin-Stokes theorems for fractional calculus are proved. The fractional Jacobian for fractal continuum flow and the Hausdorff material derivative are defined and the form of Reynolds transport theorem for fractal continuum flow is obtained. The fundamental conservation laws for fractal continuum flow are established. The gravitational head and hydrostatic pressure distributions in fractal continuum are defined. The generalized Euler equation, Bernoulli integral, and wave equations for fractal continuum flow are derived. The vector form of the generalized Navier-Stokes equation for fractal continuum flow ${}^D_3\Phi^3_D \subset E^3$ is derived. Section IV is devoted to the mapping of fluid flow in a fractally permeable medium into the fractal continuum flow ${}^D_{d_\ell}\Phi^3_D \subset E^3$. The analog of Darcy's law for fractal continuum flow is suggested and the pressure-transient equation is derived. Comparisons of the fractal continuum flow approach with other models of fluid flow in fractally permeable media and the experimental field data for reservoir tests are discussed. A brief summary and some relevant conclusions are outlined in Sec. V.

## II. FRACTAL PROPERTIES OF PERMEABLE MEDIA

Now it is widely accepted that the porosity and fractures in soils and geological formations exhibit fractal features over many length scales, ranging from the microscopic pore to field scale (see, for review, Refs. [1–7]). These include the fractal geometries of pore space or fracture networks, the fractal roughness of pore and/or fracture surfaces, and the heavy tiled distributions of pore and/or fissure sizes. A medium displaying one or more of these features we call a fractally permeable medium.

Mathematically, a fractal can be characterized by its intrinsic metric dimension associated with an appropriate intrinsic measure characterized by the intrinsic metric dimension $d_\ell$ [9], commonly called the chemical [10] or the spreading [11] dimension. This dimension quantifies how the "elementary" structural units of the fractal are "glued" together to form the entire fractal object and determines the number of independent mutually orthogonal directions on the fractal. Accordingly, the number of the independent coordinates that can be introduced

 ©2012 American Physical Society

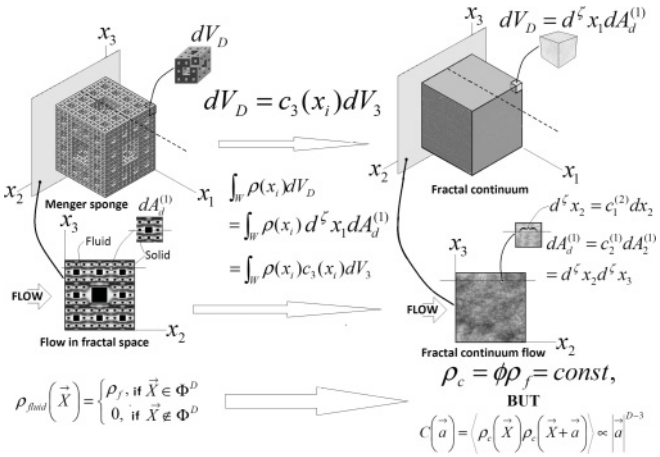


FIG. 1. Illustration of the mapping of a discontinuous prefractal Menger sponge into the fractal continuum with the mass fractal dimension $D = \ln 20/\ln 3$. Notice that the intersection of the Menger sponge with a plane is the Sierpinski carpet of the fractal dimension $d = \ln 8/\ln 3$, while the intersection of the Menger sponge with a line is the Cantor set with the fractal dimension $\alpha = \ln 2/\ln 3$, whereas the density of states along the normal to the intersection of the fractal continuum with the plane is characterized by the scaling exponent $\zeta = \ln(2.5)/\ln 3 > \alpha$.

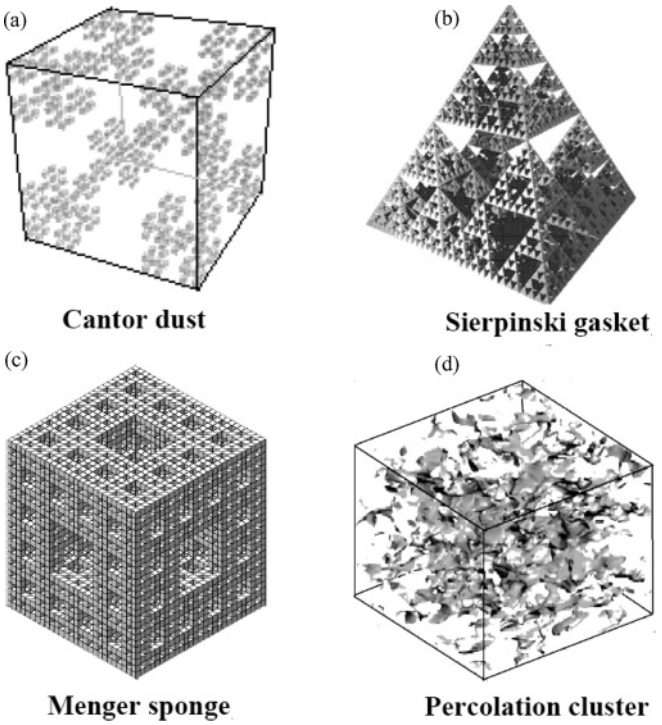


FIG. 2. Fractal models of porous media: (a) Cantor dust $D = 3\ln 2/\ln 3 = 1.89$, (b) Sierpinski gasket ($D = \ln 4/\ln 2 = 2$), (c) Menger sponge ($D = \ln 20/\ln 3 = 2.7268$), and (d) percolation cluster ($D = 2.524 \pm 0.008$). The compete sets of fractal parameters of these fractals are given in Table I.

in the fractal space is equal to $d_\ell$. In this context $d_\ell$ can be treated as a fractional analog of the Euclidean topological dimension. Although there were attempts to formally introduce a fractional number of coordinates in the fractal space (see, for example, Ref. [12]), the concept of fractional coordinates (see Refs. [13]) seems to be a more physical framework [8]. Furthermore, the dynamic properties of the fractal are governed by its spectral dimension $d_s$, which defines the Lagrangian dimension of the fractal and thus governs the density of characteristic modes of the fractal structure $\Omega(\omega) \propto \omega^{d_s-1}$ [14]. Consequently, the fractal dimension of random walk on the fractal is equal to $d_W = 2d_\ell/d_s$ [14,15].

On the other hand, the embedding of a fractal with the chemical dimension $d_\ell < n$ into Euclidean space $E^n$ is characterized by the metric dimension $D$ associated with an appropriate Euclidean measure [16] and the fractal dimension of geodesic lines on the fractal $d_{\min}$, also called the fractal dimension of the shortest (or minimum) path [14–16]. These dimensions are related to the chemical (intrinsic metric) dimension as $D = d_{\min}d_\ell$ (see Fig. 2 and Table I), while the fractal dimension of random walk on the fractal embedded in $E^n$ is $D_W = 2D/d_s = 2d_\ell d_{\min}/d_s = 2 + \theta$, where $\theta$ is the so-called anomalous diffusion exponent [11]. In the case of ordinary diffusion $\theta = 0$, whereas $\theta > 0$ and $\theta < 0$ are associated with sub- and superdiffusion, respectively [11].

It is important to note that the mathematical definitions of fractal dimension $D$ are based on the concept of fractal covering by balls or cubes of some size $\ell$, or at most $\ell$ in the limit $\ell \to 0$ [16]. In many cases, the number of covering balls (cubes) scales with $\ell$ as $N(\ell) \propto \ell^D$ [16,17]. It is precisely this scaling property that gives rise to the use of fractal concepts to model the "physical fractals," such as porous media, which can display the scaling behavior $N(\ell) \propto \ell^D$ in the bounded interval of length scale $\ell_0 < \ell < \xi$ only, where $\ell_0$ and $\xi$ are the lower and upper cutoffs of the fractal (power-law) behavior. Accordingly, the definitions of fractal dimensions for real-world systems are based on some kind of fractal quasimeasure (see [18]), rather than on a strictly metric measure. In this context, the fractal dimension of a physical fractal is commonly associated with the power-law dependence of the mass of any of its fraction $m(L)$ on the characteristic size of this fraction $L \gg \ell_0$, which can be expressed as

$$m(L) = m_0(L/\ell_0 + 1)^D, \tag{1}$$

where $m_0$ is a proportionally constant, $\ell_0$ is the lower cutoff, and $D$ is the mass fractal dimension. In the case of porous medium with a fractal geometry of the pore space, the Euclidean volume of the pore space scales with the characteristic size of fractally permeable medium fraction as

$$V_P(L) = 2^{-D}\ell_0^3(L/\ell_0 + 1)^D, \tag{2}$$

where $D$ is the mass fractal dimension of the pore space (see Refs. [2–4]).

It is imperative to emphasize that the mass fractal dimension tells us nothing about the connectivity and tortuosity of flow paths in the fractally permeable medium. In fact, fractals characterized by the same fractal dimension $D$ can have different chemicals, minimum paths, and spectral dimensions. Hence, to model a specific porous and/or fissured medium we need to know at least three independent fractional dimensions, as well as the corresponding scaling ranges. Additionally, the specific fractal geometry of a porous (fissured) medium can be characterized by another set of independent scaling exponents, such as the fractal dimension of the backbone $D_{bb}$ of the

TABLE I. Fractal characteristics of four classic fractals (see Fig. 2) widely used as models of porous media (data are taken from Refs. [10,11,16,17,19]).

| Scaling exponent | | Cantor dust in three dimensions | Three-dimensional Sierpinski gasket | Menger sponge | Percolation cluster in three dimensions |
|---|---|---|---|---|---|
| $D$ | | $3\ln 2/\ln 3 = 1.89$[a] | $2$[a] | $\ln 20/\ln 3 = 2.7268$[a] | $2.524 \pm 0.008$[b] |
| $d_\ell$ | | $3$[a] | $D = 2$[a] | $d_\ell = D$ | $1.837$[b] |
| $d_s$ | | $3$[a] | $2\ln 4/\ln 6 = 1.55$[a] | $2.51$[b] | $1.33$[b] |
| $d_{\min}$ | $D/d_\ell$ | $\ln 2/\ln 3 = 0.63$[a] | $1$[a] | $1$[a] | $1.374 \pm 0.004$[b] |
| $D_W$ | $2D/d_s$ | $D_W = 2d_{\min}$ | $\ln 6/\ln 2 = 2.58$[a] | $2.17$[b] | $3.755$[b] |
| $\theta$ | $D_W - 2$ | –0.74 | 0.58 | 0.17 | 1.755 |
| $D_{bb}$ | | | $D_{bb} = D$ | $D_{bb} = D$ | $1.87 \pm 0.03$[b] |
| $d_\ell^{bb}$ | | | $d_\ell^{bb} = D_{bb} = D$ | $d_\ell^{bb} = d_\ell$ | $1.36 \pm 0.02$[b] |
| $d_s^{bb}$ | | | $d_s^{bb} = d_s$ | $d_s^{bb} = d_s$ | $1.21$[b] |
| $D_W^{bb}$ | $2D^{bb}/d_s^{bb}$ | | $D_W^{bb} = D_W$ | $D_W^{bb} = D_W$ | $3.09 \pm 0.03$[b] |
| $D_{\text{red}}$ | | | | | $1.14 \pm 0.01$[b] |
| $D_{\text{hull}}$ | | $D_{\text{hull}} = D$ | $D_{\text{hull}} = D$ | $D_{\text{hull}} = D$ | $2.55 \pm 0.02$[b] |
| $d_i$ | | $2\ln 2/\ln 3 = 1.26$[a] | $\ln 2/\ln 3 = 0.63$[a] | $\ln 8/\ln 3 = 2.8928$[a] | $D - 1 = 1.53$ |
| $\alpha_i$ | | $\ln 2/\ln 3 = 0.63 = d_{\min} = (1/3)D$[a] | $1$[a] | $\ln 2/\ln 3 = 0.63 < D/3$ | $D - 2 = 0.53 > \alpha_i$ |
| $D - d_i$ | | $\ln 2/\ln 3 = 0.63 = \alpha_i = (1/3)D$ | $\ln(4/3)/\ln 2 = 0.415 < D/3 < \alpha_i$ | $\ln 2.5/\ln 3 = 0.834 > \alpha_i < D/3$ | $1 > D/3 > \alpha_i$ |

[a]Exact values.
[b]Results of numerical simulations.

pore space or fracture network, defined as the union of all self-avoiding random walks between two points [10,11,19], the fractal dimension $D_{\text{red}}$ of the red bonds, defined as the bonds which, when broken, divide the whole fractal into two parts, and the fractal dimension $D_{\text{hull}}$ of the hull, defined as the set of fractal sites that form the entire external perimeter, among others [11]. Besides, the fractal distribution of pore (fissure) sizes can have the heavy tail asymptotic $P \propto L^{D_{\text{dist}}}$, where $D_{\text{dist}}$ is the fractal distribution dimension, even when the pore space geometry is Euclidian (see Refs. [20]).

Regarding the transport in a fractally permeable medium it is easy to understand that that the fluid flow is controlled by the fractal dimension of the backbone $D_{bb}$ of the fracture network or pore space, rather than by the corresponding mass fractal dimension $D \geqslant D_{bb}$ [10,19]. Furthermore, the connectivity and tortuosity of flow path through a fractally permeable medium can be characterized by the backbone chemical dimension $d_\ell^{bb}$, which can be defined from the scaling behavior,

$$V_{BB} = \ell_0^{3-d_\ell^{bb}} \Lambda^{d_\ell^{bb}}, \tag{3}$$

where $V_{BB}$ is the volume of the backbone space and

$$\Lambda = 2^{-d_{\min}} \ell_0 \left( \frac{L}{\ell_0} + 1 \right)^{d_{\min}} \tag{4}$$

is the length of the shortest path between two points on the fractal divided by the distance $L$ in the embedding Euclidean space, while $V_{BB}(\ell_0) = \ell_0^3$. Notice that the geodesic lines on the fractal backbone are characterized by the same dimension of the minimum path $d_{\min}$ as the geodesic lines on the whole fractal [10]. Accordingly, the tortuosity of the shortest path, defined as the ratio $\Xi = \Lambda/L$, scales with the Euclidean distance between two points as

$$\Xi \propto \left( \frac{L}{\ell_0} \right)^{d_{\min}-1} \tag{5}$$

for $L \gg \ell_0$. Notice that for discontinuous fractals, such as Cantor dust, the fractal dimension of the shortest path can be less than one (see Fig. 2 and Table I), and so the chemical fractal dimension $d_\ell = D/d_{\min}$ is larger than the mass fractal dimension $D$ defined by Eqs. (1) or (2). On the other hand, if there is a continuous path between any two points on the fractal, the fractal dimension of the shortest path $d_{\min}^{bb} = d_{\min} \geqslant 1$, while the chemical dimension $d_\ell^{bb} \leqslant d_\ell \leqslant D$ (see Table I). Besides, a random walk on the backbone of a fractally permeable medium is characterized by the random walk dimension

$$D_W^{bb} = 2 + \theta_{bb} = \frac{2D_{bb}}{d_s^{bb}} \leqslant D_W, \tag{6}$$

where $d_s^{bb}$ is the spectral dimension of the backbone and $\theta_{bb}$ is the exponent characterizing an anomalous diffusion on the backbone (see Refs. [10,11,19] and Table I). It is pertinent to point out that while $\theta$ is frequently considered as an intrinsic property of the fractal, in fact, however, it is allied with the mechanism of the diffusion process. Specifically, in the case of continuous Darcian flow through a fractal the anomalous diffusion exponent is $\theta = 0$ ($d_s = D$, or $d_s = D_{bb}$, if $D_{bb} < D$ and so $D_W^{\text{Darcian}} \equiv 2$), even when the random walk on the fractal is characterized by $\theta > 0$, and so $D_W > 2$ (see Table II).

The fluid flow in a fractally permeable medium is also dependent on the fractal dimension of the pore (fracture) surfaces $D_S$ and the fractal dimensions $d_i$ of backbone intersections with the two-dimensional Cartesian planes perpendicular to coordinate axis $i = 1,2,3$ (see [8]). Specifically,

TABLE II. Fractal properties of porous medium and the corresponding fractal continua.

| Fractal porous medium ($\Phi^D$) | | Fractal continuum | | | |
|---|---|---|---|---|---|
| Property | Scaling exponent | Characteristic | Continuum flow ${}^{D}_{3}\Phi^3_D \subset E^3$ | Continuum flow ${}^{D}_{d_\ell}\Phi^3_D \subset E^3$ | Diffusion ${}^{d_s}_{d_\ell}\Phi^3_D \subset E^3$ |
| Mass scaling | $D$ | Fractal metric | Fractal mass dimension associated with the box-counting quasimeasure Eqs. (8)–(10) | | |
| Connectivity | $d_\ell$ | Topology | $d_\ell = 3$ | Fractional topological dimension of fractal continuum [see Eqs. (23) and (24)] | |
| Shortest paths scaling | $d_{\min} = D/d_\ell$ | Tortuosity | Accounted in constitutive laws | | |
| Intersection with plane | Fractal dimensions of intersections $d_i$ $i = 1,2,3$ | Density of states on the intersection with Cartesian plane $(x_j,x_k)$ | Fractal dimension of fractal continuum intersection with Cartesian plane $(x_j,x_k)$ | | |
| Intersection with line | Fractal dimension of intersection $D - d_i$ | $\zeta_i = D - d_i$ | Not defined | | |
| | | Density of states in the direction of the normal to intersection with Cartesian plane $(x_j,x_k)$ | Order of the Hausdorff derivative (19) | | |
| Roughness of pore and/or fracture surfaces | $D_S$ | Permeability (resistance) | Accounted in constitutive laws | | |
| Spectral dimension | $d_s = 2D/D_W = \frac{2D}{2+\theta}$ [a] | Dimension of Lagrangian [14] | $d_s = D$ [b] | | Order of the Hausdorff time derivative [see Eqs. (35) and (36)] |

[a]Alexander-Orbach law [41] associated with the fractal Einstein law related the electrical resistivity exponent to the fractal dimensions of medium and random walk $\vartheta = D_W - D$ [42].
[b]In the case of Darcian fractal continuum flow the Alexander-Orbach law fails, while $d_s = D$, such that the fractal Einstein law obeys the generalized form $\vartheta = 0.5 D_W (2 - D)$ (see Ref. [44]).

the fractal dimension $D_S$ governs the medium permeability (see Refs. [21]), whereas the fractal dimension $d_i$ controls the Darcian velocities (volume of liquid flowing per unit area per unit time) in a fractally permeable medium. Although there are many isotropic fractals obeying the so-called Mandelbrot's rule of thumb for intersections according to which the fractal dimension of intersection between the fractal and a two-dimensional plane is equal to

$$d = D - 1 \tag{7}$$

for any intersection with the two-dimensional plane (e.g., see Table I and Refs. [17,22]), more generally, the fractal dimensions of intersections $0 < d_i \leqslant 2$ are independent characteristics of a specific fractally permeable isotropic or anisotropic medium (e.g., see Figs. 1 and 2, Table I, and Refs. [8,16]).

## III. THE CONCEPT OF FRACTAL CONTINUUM FLOW

The aim of the fractal continuum approach consists of the mapping of an intrinsically discontinuous fractal medium into the fractal continuum model (see Fig. 1), the behavior of which is describable within a continuum framework [8]. Strictly speaking, a fractal $\Phi^D$ with $D < 3$ cannot continuously fill the embedding Euclidean space $E^3$. Still, we can define the three-dimensional fractal continuum ${}^{d_s}_{d_\ell}\Phi^3_D \subset E^3$ accounting the fractal metric, topology, and dynamic properties of the modeled fractal medium $\Phi^D$. In this way, in Ref. [8] the fractal continuum $\Phi^3_D \subset E^3$ was defined as a three-dimensional region of Euclidean space $E^3$ filled with continuous matter (leaving no pores or empty spaces) such that its properties, for example, density $\rho(x_i)$, displacements $v_j(x_i)$, etc., are describable by the continuous (or, at worst, piecewise continuous) and differentiable functions of the of the space and time variables, whereas the mass of any cubic (or spherical) region $W \subset \Phi^3_D$ of size $L$ obeys the fractal scaling law (3) with the mass fractal dimension $D$ related to some kind of box-counting quasimeasure. This definition tells nothing about the topology and dynamic properties of fractal continuum, because in Ref. [8] it was implicitly assumed that the fractal continuum $\Phi^3_D$ is characterized by the chemical dimension $d_\ell = 3$, while the spectral dimension is $d_s = D$, and so $\Phi^3_D \equiv {}^D_3\Phi^3_D$. Below, the concept of fractal continuum flow is generalized for the case of arbitrary values of $d_\ell$ and $d_s$.

### A. Fractal metric of fractal continua

The above definition of fractal continuum $\Phi^3_D \subset E^3$ implies that the mass of region $W \subset \Phi^3_D$ should be defined as

$$m = \int_W \rho(x_i) dV_D = \int_W \rho(x_i) c_3(x_i, D) dV_3 \propto L^D, \tag{8}$$

where $dV_3(dx_i)$ is the infinitesimal volume element in $E^3$, while $dV_D = c_3(x_i, D) dV_3$ is the infinitesimal volume element of $\Phi^3_D \subset E^3$, such that the function providing transformation between the Euclidean and fractal quasimeasures is defined as

$$c_3(x_i, D) = dV_D / dV_3. \tag{9}$$

Physically, function $c_3(x_i, D)$ plays the role of density of states in the fractal continuum, that is, describes how permitted states of particles forming the fractal continuum are closely packed in the Euclidean space (see Ref. [23]). The symmetry and functional form of the transformation function are determined by the symmetry of the fractal under consideration [8]. Generally, the infinitesimal volume element of $\Phi^3_D$ can be presented in the following form:

$$dV_D = d^\zeta x_k dA^{(k)}_d(x_{i\neq k}), \tag{10}$$

where $dA^{(k)}_d = c^{(k)}_2(x_{i\neq k}, d_k) dA^{(k)}_2$ is the infinitesimal area element on the intersection of fractal continuum with the Cartesian plane $(x_i, x_j) \in E^2$ normal to axes $k$ in $\Phi^3_D$ and $dA^{(k)}_2$ is the infinitesimal area of this element in $E^2$, while the transformation function $c^{(k)}_2(x_{i\neq k}, \ell_{i\neq k}, d_k) = dA^{(k)}_d / dA^{(k)}_2$ represents the density of states on the intersection; $d^\zeta x_k = c^{(k)}_1(x_k, \zeta_k) dx_k$ is the infinitesimal length element along a normal to the intersection and $c^{(k)}_1(x_k, \zeta_k)$ is the density of states along this direction [8].

In the case of homogeneous fractal continuum

$$\rho(x_i) = \rho_c = \text{const}, \tag{11}$$

and so from Eqs. (9) and (10) follows that the density of states in the homogeneous fractal continuum can be represented in the following form:

$$c_3(x_i, D) = \ell_k^{\zeta_k - 1} (x_k/\ell_k + 1)^{\zeta_k - 1} c^{(k)}_2(x_{i\neq k}, \ell_{i\neq k}, d_k), \tag{12}$$

where $\ell_i$ is the lower cutoff along the Cartesian axis $i$ and the scaling exponent $\zeta_k$ characterizing the density of states along the direction of the normal to the intersection is defined as

$$\zeta_k = D - d_k, \tag{13}$$

such that, generally,

$$\sum_i^3 \zeta_i \neq D; \tag{14}$$

for example, in the case of fractal continuum obeying the Mandelbrot's rule of thumb (7), for example, the percolation cluster in 3D [see Fig. 2(d)], the sum $\sum_i^3 \zeta_i = 3 > D$, whereas in the case of the Menger sponge [see Fig. 2(c)], the sum $\sum_i^3 \zeta_i = 2.5021 < D = 2.7268$ (see Table I and Ref. [8]).

Equations (8)–(13) define the fractal metric of fractal continuum, which is independent on the fractal dimensions $d_\ell$ and $d_s$. Accordingly, here we assume that fractal continua ${}^{d_s}_{d_\ell}\Phi^3_D \subset E^3$ with different $d_\ell$ and $d_s$ are characterized by the same fractal metric defined by Eqs. (8)–(13), whereas the fractal continuum topology and dynamics are characterized by $d_\ell$ and $d_s$, respectively. Furthermore, it is pertinent to note that, regardless of the homogeneity of the fractal continuum expressed by Eq. (11), the density distribution in $E^3$ displays the long-range correlations characterized by the power-law scaling behavior of the density-density correlation function

$$\begin{aligned} C(a) &= \langle \rho(\vec{x}) \rho(\vec{x} + \vec{a}) \rangle \\ &= V_3^{-1} \int_W \rho(\vec{x}) \rho(\vec{x} + \vec{a}) c_3(\vec{x}, D) dV_3 \propto |\vec{a}|^{D-3} \end{aligned} \tag{15}$$

for $|\vec{a}| \gg \ell_0$, where $\vec{a} \in E^3$ and the brackets denote the spatial average. It is easy to understand that any space independent

property of the fractal continuum possesses the same kind of long-range correlations.

### B. Fractional calculus in fractal continua

To describe the kinematics and dynamics of fractal continua ${}^{d_s}_{d_\ell}\Phi^3_D \subset E^3$ we need to define an appropriate fractional calculus linked to the fractal metric defined by Eqs. (8)–(13) and accounting for the topology and dynamic properties of the fractal continuum flow. In this way, we noted that the right-hand side integral in Eq. (8) with the transformation function $c_3(x_i)$ defined by Eq. (12) represents the multivariate Riemann-Liouville fractional integral up to a constant numerical factor (see Ref. [8]). The nonlocal fractional derivatives are also commonly employed when dealing with fractals (see, for example, Refs. [24]). One of the principal stimuli to the use of the nonlocal differential operators is a nondifferentiability of fractal functions. However, this is not the case with fractal continuum ${}^{d_s}_{d_\ell}\Phi^3_D$, the properties of which are continuous differentiable functions in the Euclidean space $E^3$. This permits the use of local differential operators related to some kind of a local fractional derivative inverse to the Riemann-Liouville fractional integral employed in the definition of the fractal continuum.

There are several definitions of local fractional derivatives (see, for review, [25] and references therein). In most of them, the local fractional derivative $d^\alpha f/dx^\alpha$ is introduced as a special case of the nonlocal fractional derivative, for example, in the limit $x \to y$, where $y$ is the upper (or lower) limit of the fractional integral used to define the corresponding nonlocal fractional derivative. While the local fractional derivative defined in such way is automatically inverse to the corresponding fractional integral, the expression of associated local fractional operators in terms of ordinary derivatives is somewhat complicated and does not always exist.

At the same time, in Refs. [26,27] the local Laplacian operator in $E^n$ was generalized for the Euclidean space $E^\alpha$ with the fractional topological dimension $\alpha$. Specifically, in Ref. [26] the local fractional Laplacian operator in $E^\alpha$ was defined as

$$\nabla^2_D = \frac{\partial^2}{\partial r^2} + \frac{D-1}{r}\frac{\partial}{\partial r} + \frac{1}{r^2}\left[\frac{\partial^2}{\partial \vartheta^2} + \frac{D-2}{\tan\vartheta}\frac{\partial}{\partial \vartheta}\right], \tag{16}$$

where the angles $\vartheta$ is measured relative to any axis in the fractional space passing through the origin. This definition was generalized in Ref. [27] to three orthogonal coordinates as

$$\begin{aligned}\nabla^2_D &= \sum_i^3 \left(\frac{\partial^2}{\partial x_i} + \frac{\alpha_i - 1}{x_i}\frac{\partial}{\partial x_i}\right)\\ &= \sum_i^3 \frac{1}{x_i^{\alpha_i - 1}}\frac{\partial}{\partial x_i}\left(x_i^{\alpha_i - 1}\frac{\partial}{\partial x_i}\right),\end{aligned} \tag{17}$$

where $\alpha_i \leqslant 1$ are the topological exponents along the Cartesian axes $i = 1,2,3$ in $E^3$, such that $\sum_i^3 \alpha_i = \alpha \leqslant 3$. It is pertinent to note that the generalized Laplacian (17) can be linked to the topology of the fractal continuum ${}^{d_s}_{d_\ell}\Phi^3_D \subset E^3$ characterized by the chemical fractal dimension $d_\ell$, rather than to its metric defined by Eqs. (8)–(13).

On the other hand, quite recently, the authors of [28] have introduced the concept of Hausdorff derivative defined as follows:

$$\frac{d^H}{dx^\zeta} f = \lim_{x \to x'} \frac{f(x') - f(x)}{x'^\zeta - x^\zeta}. \tag{18}$$

It is easy to see that Eq. (18) can be presented in the form of ordinary derivative multiplied by a power-law function of $x$. Furthermore, rewriting Eq. (18) in the form

$$\begin{aligned}\frac{d^H}{dx^\zeta} f &= \lim_{\Delta x \to 0} \frac{\zeta\, \Delta f(x)}{\ell_0 \Delta(x/\ell_0 + 1)^\zeta}\\ &= \lim_{\Delta x \to 0} \frac{\Delta f(x)}{\Delta x}\frac{\zeta}{\ell_0 \Delta(x/\ell_0 + 1)^\zeta/\Delta x}\\ &= \zeta \ell_0^{-1}\left[\frac{d(x/\ell_0 + 1)^\zeta}{dx}\right]^{-1}\frac{d}{dx} f\\ &= \left(\frac{x}{\ell_0} + 1\right)^{1-\zeta}\frac{d}{dx} f = \frac{\ell_0^{\zeta-1}}{c_1}\frac{d}{dx} f = \frac{d}{d^\zeta x} f,\end{aligned} \tag{19}$$

it is straightforward matter to verify that Hausdorff derivative (19) is inverse to the fractional integral $\int f d^\zeta x = \int f c_1 dx$, where the density of states along the $x$ axis $c_1(x_i)$ is defined as in Eq. (12). Accordingly, in Ref. [8] the fractional (Hausdorff) partial derivative was defined in the following form:

$$\nabla^H_k = \left(\frac{x_k}{\ell_k} + 1\right)^{1-\zeta_k}\frac{\partial}{\partial x_k}, \tag{20}$$

where the exponents $\zeta_k$ are defined by Eq. (13). Therefore, the fractional Laplacian for the fractal continuum ${}^D_3\Phi^3_D$ can be defined as follows:

$$\begin{aligned}\Delta_H \psi &= \nabla^H_i \nabla^H_i \psi\\ &= \sum_i^3 (\chi^{(i)})^2 \left[\left(\frac{\partial^2 \psi}{\partial x_i^2}\right) + \frac{1-\zeta_i}{x_i + \ell_i}\left(\frac{\partial \psi}{\partial x_i}\right)\right],\end{aligned} \tag{21}$$

where

$$\chi^{(i)} = \ell_i^{\zeta_i - 1}/c_1^{(i)}(x_i) = (x_i/\ell_i + 1)^{1-\zeta_i}, \tag{22}$$

while the scaling exponents $\zeta_i$ are defined by Eq. (13). Notice that the dimensions of the Hausdorff derivative (19), Hausdorff partial derivative (20), and Laplacian (21) are the same as of the conventional ones, that is, $[d^H/dx^\zeta] = [L^{-1}]$, $[\nabla^H_i] = [L^{-1}]$ and $[\Delta_H] = [L^{-2}]$, respectively.

It is important to point out the difference between the Hausdorff Laplacian (21) and the fractional Laplacian (17), although both are converted in the conventional Laplacian in the Euclidean limit $\zeta_i = \alpha_i = 1$. This difference arises from different origins of these Laplacians associated with the fractional metric and fractional topology, respectively (see Table II). In this context, it is straightforward to introduce the generalized fractional Laplacian for the generalized fractal continuum ${}^{d_s}_{d_\ell}\Phi^3_D \subset E^3$ with the chemical dimension

$$d_\ell = \sum_i^3 \alpha_i = \alpha \leqslant 3 \tag{23}$$

in the following form:

$$\Delta_D^H \psi = \sum_i^3 (\chi^{(i)})^2 \left[ \left( \frac{\partial^2 \psi}{\partial x_i^2} \right) + \frac{\alpha_i - D + d_i}{x_i + \ell_i} \left( \frac{\partial \psi}{\partial x_i} \right) \right], \tag{24}$$

accounting the fractal topology, as well as the fractal metric of the fractal continuum ${}^{d_s}_{d_\ell}\Phi_D^3 \subset E^3$. Notice that when $d_\ell = 3$, the generalized Laplacian (24) is converted in the Hausdorff Laplacian (21), whereas when $D - d_i = 1$ for all $i$, while $d_\ell < 3$, the fractional Laplacian (24) is converted in the fractional Laplacian (17).

Although the definition of the generalized Laplacian (24) is somewhat speculative, it is based on the same phenomenology as the introduction of the fractional Laplacian (17) in the fractional Euclidean space (see Refs. [26,27]). Unfortunately, we cannot define the local fractional derivative allied with the generalized Laplacian (24). Even though in the case of generalized fractal continuum flow ${}^{d_s}_{d_\ell}\Phi_D^3 \subset E^3$ we can use the local fractional differential operators associated with the fractal metric defined by Eqs. (8)–(13), the generalized Laplacian (24) can be used to construct the constitutive laws for fractal continuum flows ${}^{d_s}_{d_\ell}\Phi_D^3 \subset E^3$ with different topologies characterized by the chemical dimension $d_\ell \neq D$ (see Table II).

It is straightforward to verify that the partial Hausdorff derivatives (20) obey the rule $\nabla_i^H(\psi\varphi) = \psi\nabla_i^H\varphi + \varphi\nabla_i^H\psi$ and $\nabla_i^H \mathrm{const} = 0$. Furthermore, we can construct the local fractional (Hausdorff) operators for vector calculus on the fractal continuum. Specifically, a fractional (Hausdorff) nabla operator is defined as follows:

$$\vec{\nabla}^H = \vec{e}_1 \chi^{(1)} \frac{\partial}{\partial x_1} + \vec{e}_2 \chi^{(2)} \frac{\partial}{\partial x_2} + \vec{e}_3 \chi^{(3)} \frac{\partial}{\partial x_3}, \tag{25}$$

where $\vec{e}_i$ are base vectors. Accordingly, the Hausdorff gradient can be defined as the nabla operator (25) applied to a scalar function $\psi(x_i)$ as

$$\mathrm{grad}_H \psi = \vec{\nabla}^H \psi = \left(\nabla_1^H \psi\right)\vec{e}_1 + \left(\nabla_2^H \psi\right)\vec{e}_2 + \left(\nabla_3^H \psi\right)\vec{e}_3, \tag{26}$$

while the Hausdorff divergence of vector field $\vec{\Psi} = (\psi_1, \psi_2, \psi_3)$ can be defined as the scalar product

$$\mathrm{div}_H \vec{\Psi} = \vec{\nabla}^H \cdot \vec{\Psi} = \sum_i^3 \nabla_i^H \Psi_i, \tag{27}$$

where the symbol "$\cdot$" denotes the scalar product. Notice that the Hausdorff divergence represents the ratio of total flux through a closed surface to the fractal continuum enclosed by the surface when the volume shrinks toward $\ell_0^3$. This leads to definition of the Hausdorff curl operator of a vector field in the following form:

$$\mathrm{rot}_H \vec{\Psi} = \vec{\nabla}^H \times \vec{\Psi}, \quad \text{or} \quad \nabla_i^H \Psi_j = \varepsilon_{kij} \nabla_i^H \Psi_j, \tag{28}$$

where the symbol $\times$ denotes the vector product and $\varepsilon_{ijk}$ is the Levi-Civita symbol.

Now it is straightforward matter to verify that Hausdorff operators (24)–(28) obey the identities which resemble the fundamental identities of the conventional vector calculus. Namely,

$$\mathrm{div}_H \mathrm{rot}_H \vec{\Psi} = \vec{\nabla}^H \cdot (\vec{\nabla}^H \times \vec{\Psi}) = 0, \tag{29}$$

$$\mathrm{rot}_H \mathrm{grad}_H \psi = \vec{\nabla}^H \times (\vec{\nabla}^H \psi) = 0, \tag{30}$$

$$\mathrm{div}_H \mathrm{grad}_H \psi = \vec{\nabla}^H \cdot \vec{\nabla}^H \psi = \Delta_H \psi, \tag{31}$$

where the Hausdorff Laplacian operator $\Delta_H$ is defined by Eq. (21), while the Hausdorff Laplacian of a vector field is defined as

$$\begin{aligned} \Delta_H \vec{\Psi} &= (\Delta_H \psi_i)\vec{e}_1 + (\Delta_H \psi_j)\vec{e}_2 + (\Delta_H \psi_k)\vec{e}_3 \\ &= \mathrm{grad}_H \mathrm{div}_H \vec{\Psi} - \mathrm{rot}_H \mathrm{rot}_H \vec{\Psi}. \end{aligned} \tag{32}$$

Accordingly, the generalization of the Green-Gauss divergence theorem for fractal continuum reads as

$$\begin{aligned} &\int_A \vec{\Psi} \cdot \vec{n} dA_d \\ &= \int_A \Psi_k n_k dA_d^{(k)} = \int_A \Psi_k c_2^{(k)}(x_{i\neq k}, d_k) dA_2^{(k)} \\ &= \int_W c_2^{(k)}(x_{i\neq k}, \ell_{i\neq k}, d_k) \frac{\partial \Psi_k}{\partial x_k} dV_3 \\ &= \int_W c_3^{-1}(x_i/\ell_i, D_M) c_2^{(k)}(x_{i\neq k}, \ell_{i\neq k}, d_k) \frac{\partial \Psi_k}{\partial x_k} dV_D \\ &= \int_W \nabla_k^H \Psi_k dV_D = \int_W \mathrm{div}_H \vec{\Psi} dV_D, \end{aligned} \tag{33}$$

where $\vec{\Psi} = \Psi_k \vec{e}_k$ is any vector field accompanied by fractal flow, while $\vec{n} = n_k \vec{e}_k$ is a vector of normal. Furthermore the Kelvin-Stokes theorem, which relates the surface integral of the curl of a vector field $\vec{f}$ over a surface $A$ in Euclidean three-dimensional space to the line integral of the vector field over its boundary $\partial A$, can be generalized for the fractal continuum flow as

$$\begin{aligned} &\oint_{\partial A} \vec{f} \cdot \overrightarrow{dx}^{(\zeta)} \\ &= \oint_{\partial A} f_k dx_k^{(\zeta)} = \int_{\partial A} c_1^{(k)} f_k dx_k = \int_A n_k \varepsilon_{kji} \nabla_j^H \left(c_1^{(i)} f_i\right) \\ &= \int_A \vec{n} \cdot \mathrm{rot}_H \vec{f} dA_d. \end{aligned} \tag{34}$$

It should be pointed out that while formally Eqs. (33) and (34) are similar to those derived in Refs. [29,30] for an isotropic fractal continuum [31], the local fractional operators used in Eqs. (33) and (34) are substantially different from the corresponding fractional operators used in Refs. [29,30]. In this context it is pertinent to note that a general Stokes theorem for nonsmooth chains was proved in Ref. [32]. The Green-Gauss divergence and Kelvin-Stokes theorems for domains with boundaries of noninteger box dimension were proved in Refs. [33]. The fractional generalizations of Green-Gauss divergence and the Kelvin-Stokes theorem for nonlocal calculus were suggested in Refs. [34].

The Lagrangian metric of fractal continuum ${}^{d_s}_{d_\ell}\Phi_D^3 \subset E^3$ can be accounted by using the Hausdorff partial time derivative

defined as

$$\nabla_t^H = \chi_\tau(t)\frac{\partial}{\partial t}, \tag{35}$$

where $\tau_0$ is the characteristic time scale and

$$\chi_\tau = \left(\frac{t}{\tau_0}+1\right)^{1-\alpha_\tau}, \tag{36}$$

while the fractal dimension of time scale is defined as

$$\alpha_\tau = \frac{d_s}{D} = \frac{2}{D_W} = \frac{2}{2+\theta}, \tag{37}$$

where $D_W$ is the fractal dimension of random walk in the fractal continuum ${}^{d_s}_{d_\ell}\Phi^3_D \subset E^3$.

### C. Kinematics and dynamics of fractal continua

The mathematical description of fractal continuum flow ${}^{d_s}_{d_\ell}\Phi^3_D \subset E^3$ requires two sets of variables: a set for the flow domain in the Euclidean space $E^3$ and time, called independent variables, and a set for the flow phenomena taking place in the fractional space-time domain, called dependent variables. The independent variables can be established in various ways. One can look at a region of space (Euler) or look at what happens to specific pieces of the fractal continuum (Lagrange). The material or Lagrangian description is the natural choice for the setup of the basic laws for mass, momentum, and energy, whereas the spatial or Eulerian description is the most convenient framework for the solution of the associated initial and boundary value problems. Each description leads to a set of, at most, four independent variables and the basic laws appear in different form in different descriptions. In this context, the kinematic information on a fractal flow field can be given in terms of the position field or the velocity field. The velocity field does not track the behavior of individual partials, but it describes the velocity of whatever happens to be at a given location. In contrast to this, the acceleration appears more naturally in the material description as the time rate of change of the velocity of a fixed material point.

Here, we suppose that the three-dimensional fractal continuum occupies at time $t = 0$ a region $W_0 \in {}^{d_s}_{d_\ell}\Phi^3_D \subset E^3$ and, at time $t > 0$, occupies a region $W_t \in {}^{d_s}_{d_\ell}\Phi^3_D \subset E^3$, where regions $W_0$ and $W_t$ are assumed to be bounded, open, and connected. The motion of fractal continuum is determined by the position $\vec{x}$ of the material points in Euclidean space $E^3$ as a function of the reference position $\vec{x} \in E^3$ and the time $t$. Hence, $\vec{x} = \vec{\Theta}(\vec{x},t)$, where the function $\vec{\Theta}$ is defined as the mapping $W_0 \to \vec{\Theta}(W_0,t) = W_t$, and so the displacement vector

$$\vec{v} = \vec{\Theta}(\vec{x},t) - \vec{x} \tag{38}$$

describes the displacement field in the initial (reference) configuration of the fractal continuum. Further, as in the case of classical continuum mechanics, we assume that for every $t > 0$, function $\vec{\Theta}$ is a smooth one-to-one map of every material point of $W_0$ onto $W_t$, such that there exists a unique inverse of (38), at least locally, if and only if the determinant of the fractal Jacobian matrix defined as

$$J_D^{(ij)} = \left[\nabla_i^H X_j\right] = \begin{vmatrix} \nabla_1^H X_1 & \nabla_2^H X_1 & \nabla_3^H X_1 \\ \nabla_1^H X_2 & \nabla_2^H X_2 & \nabla_3^H X_2 \\ \nabla_1^H X_3 & \nabla_2^H X_3 & \nabla_3^H X_3 \end{vmatrix} \tag{39}$$

is not identically zero, that is,

$$0 < J_D = \det J_D^{(ij)} = \varepsilon_{ijk}\nabla_1^H X_i \nabla_2^H X_j \nabla_3^H X_k < \infty, \tag{40}$$

where $\varepsilon_{ijk}$ is the Levi-Civita permutation symbol. Notice that the matrix in Eq. (39) is nothing other than the Hausdorff deformation gradient in the fractal continuum ${}^{d_s}_{d_\ell}\Phi^3_D \subset E^3$, while the Jacobian (40) depends only on the fractal metric, but not on the fractal continuum topology characterized by $d_\ell$. This is easy to understand since $J_D$ measures the local change of volume only, such that a deformation conserves the volume of a region $W \subset {}^{d_s}_{d_\ell}\Phi^3_D$, if and only if $J_D = 1$.

In this context, the velocity of fractal continuum flow $W \subset {}^{d_s}_{d_\ell}\Phi^3_D$ can be defined using either the intrinsic (fractal) or natural time scale. In the former case, the particle velocity can be defined as

$$\vec{v} = \nabla_t^H \vec{v}, \tag{41}$$

where the Hausdorff time derivative is defined by Eqs. (35)–(37). Furthermore, using the conventional rule for determinant differentiating it is straightforward to obtain the generalized Euler's identity for the fractal continuum ${}^{d_s}_{d_\ell}\Phi^3_D \subset E^3$ in the following form:

$$\nabla_t^H J_D = J_D \nabla_i^H v_i. \tag{42}$$

Accordingly, we can define the fractal material fractional time derivative as

$$\left(\frac{d}{d^H t}\right)_D \psi = \nabla_t^H \psi + v_k \nabla_k^H \psi = \chi_\tau \frac{\partial}{\partial t}\psi + v_k \chi^{(k)} \frac{\partial}{\partial x_k}\psi, \tag{43}$$

where $\psi(x_i,t)$ is any quantity accompanied by a moving region $W_t \subset {}^{d_s}_{d_\ell}\Phi^3_D$, such that the generalization of the Reynolds transport theorem for a fractal continuum ${}^{d_s}_{d_\ell}\Phi^3_D \subset E^3$ will reads as follows:

$$\begin{aligned}
&\left(\frac{d}{d^H t}\right)_D \int_{W_t} \psi dV_D \\
&= \left(\frac{d}{d^H t}\right)_D \int_{W_0} \psi J_D dV_D^0 \\
&= \int_{W_0} \left[\left(\frac{d}{d^H t}\right)_D \psi J_D + \psi \left(\frac{d}{d^H t}\right)_D J_D\right] dV_D^0 \\
&= \int_{W_0} \left[\left(\frac{d}{d^H t}\right)_D \psi + \psi \nabla_k^H v_k\right] J_D dV_D^0 \\
&= \int_{W_t} \left[\left(\frac{d}{d^H t}\right)_D \psi + \psi \nabla_k^H v_k\right] dV_D \\
&= \int_{W_t} \left(\nabla_t^H \psi + \nabla_k^H (\psi v_k)\right) dV_D \\
&= \int_{W_t} \left(\nabla_t^H \psi\right) dV_D + \int_A \psi v_k n_k dA_d^{(k)}.
\end{aligned} \tag{44}$$

Notice that in the case of fractal continuum $\Phi_D^3 \equiv {}_3^D\Phi_D^3 \subset E^3$, Eqs. (41)–(44) are converted into the corresponding equations derived in Ref. [8] and further into the conventional equations for Euclidean continua, if the equality (7) holds.

Here, it should be pointed out that the use of an intrinsic (fractal) time scale is justified when we describe an anomalous diffusion of fractal continuum, but not when the fractal continuum flow is used to model the fluid flow in a fractal porous medium. In fact, anomalous values of $D_W$ reflect that the walking particle can visit the same place many times, but this is not the case of Darcian flow in a porous medium. Hence, to model the Darcian flow in porous media we should assume that the fractal continuum flow is characterized by the spectral dimension $d_s = D$, rather than by the spectral dimension of fractal porous medium (see Table II). Moreover, in the next section we show that the use of fractional time derivative leads to failure of the momentum conservation, which is essential for the fluid flow, but not for the diffusion. Therefore, the fractal continuum flow velocity should be defined as

$$\vec{u} = \frac{\partial}{\partial t}\vec{v} \tag{45}$$

and so the Euler's identity for the fractal continuum ${}_{d_\ell}^D\Phi_D^3 \subset E^3$ reads as

$$\left(\frac{d}{dt}\right)_D J_D = J_D \nabla_i^H \upsilon_i, \tag{46}$$

where the fractal material time derivative is defined as

$$\left(\frac{d}{dt}\right)_D \psi = \frac{\partial \psi}{\partial t} + u_k \nabla_k^H \psi, \tag{47}$$

and the Reynolds transport theorem for a fractal continuum has the following form:

$$\begin{aligned}
&\left(\frac{d}{dt}\right)_D \int_{W_t} \psi dV_D \\
&= \left(\frac{d}{dt}\right)_D \int_{W_0} \psi J_D dV_D^0 \\
&= \int_{W_0} \left[\left(\frac{d}{dt}\right)_D \psi J_D + \psi \left(\frac{d}{dt}\right)_D J_D\right] dV_D^0 \\
&= \int_{W_0} \left[\left(\frac{d}{dt}\right)_D \psi + \psi \nabla_k^H u_k\right] J_D dV_D^0 \\
&= \int_{W_t} \left[\left(\frac{d}{dt}\right)_D \psi + \psi \nabla_k^H u_k\right] dV_D \\
&= \int_{W_t} \left(\frac{\partial}{\partial t}\psi + \nabla_k^H(\psi u_k)\right) dV_D \\
&= \int_{W_t} \frac{\partial}{\partial t}\psi dV_D + \int_A \psi u_k n_k dA_d^{(k)},
\end{aligned} \tag{48}$$

which implies that a rate of change of the integral of a function over a volume of fractal continuum is related to the change in the value of the function in the volume and any change in the size of the volume due to the movement of its boundaries. Notice the difference between Eqs. (47) and (48) and the forms of the material time derivative and the Reynolds transport theorem adopted in the fractal continuum model suggested in Refs. [35].

### D. Conservation laws for fractal continuum flow

In previous Rapid Communication [8] the fundamental conservation laws were derived for the special case of fractal continua $\Phi_D^3 \equiv {}_3^D\Phi_D^3 \subset E^3$. It is straightforward to see that a specific fractal topology of generalized fractal continuum flow ${}_{d_\ell}^D\Phi_D^3 \subset E^3$ does not affect the fundamental balance equations (see Sec. III C). Specifically, the continuity equation for the fractal continuum flow ${}_{d_\ell}^D\Phi_D^3 \subset E^3$ can be written in the form

$$\frac{\partial \rho_c}{\partial t} = -\mathrm{div}_H(\rho_c \vec{u}), \tag{49}$$

which implies that the velocity field in a stationary flow ($\vec{u} =$ const) of an incompressible ($\rho_c =$ const) fractal continuum is solenoidal in the sense that for any closed surface $\partial W$ the net total flux through the fractal surface is equal to zero when

$$\mathrm{div}_H \vec{u} = 0, \quad \text{whereas } \mathrm{div}\vec{u} = \sum_i^3 \frac{\partial u_i}{\partial x_i} \neq 0. \tag{50}$$

It is pertinent to point out that the solenoidal velocity field in the fractal continuum can be expressed as the Hausdorff curl of a vector potential $\vec{\Phi}$, that is, $\vec{u} = \mathrm{rot}_H \vec{\Phi}$, where the Hausdorff curl is defined by Eq. (28). In this context, the irrotational flow of fractal continuum should be defined as the flow with $\mathrm{rot}_H \vec{u} = 0$. Making use of the terminology of classical hydrodynamics, the vector field

$$\vec{\omega} = \mathrm{rot}_H \vec{u} \tag{51}$$

can be termed as the fractal vorticity. Furthermore, using identities of fractional vector calculus (29)–(32), the velocity of irrotational flow of fractal continuum can be presented as $\vec{u} = \mathrm{grad}_H \psi$, where the scalar field $\psi(x_i)$ obeys the condition $\Delta_H \psi = 0$. It is straightforward to verify that any velocity field in fractal continuum can be decomposed into irrotational and solenoidal parts as follows:

$$\vec{u} = \mathrm{rot}_H \vec{\Phi} + \mathrm{grad}_H \psi. \tag{52}$$

Notice that in the case of fractal continuum flow obeying Mandelbrot's rule of thumb for intersections (7), Eq. (52) coincides with the decomposition used in classical hydrodynamics.

The conservation of momentum is Newton's second law. Following to the concepts of classical continuum mechanics, the forces that act on the fractal continuum or its part can be divided into two categories: those that act by contact with the surface, called surface tractions ($\vec{T}$), and those that act at a distance, called the volume or body forces ($\vec{F}$). Further, taking into account the definition of the fractal Jacobian (39), the surface forces in the fractal continuum flow can be presented as the Hausdorff gradient (26) of stresses, that is,

$$\vec{T} = -\nabla_i^H \sigma_{ij}, \tag{53}$$

where $\sigma_{ij} = p\delta_{ij} - \sigma_{ij}^v$ is the Cauchy stress tensor, $p$ is the pressure, and $\sigma_{ij}^v$ is the viscosity stress tensor. The conservation of momentum in fractal continuum flow ${}_{d_\ell}^D\Phi_D^3 \subset E^3$ implies that

$$\left(\frac{d}{dt}\right)_D \int_W \rho_c u_i dV_D = \int_W \left(\rho_c f_i + \nabla_j^H \sigma_{ij}\right) dV_D, \tag{54}$$

where $f_i$ is the density of volume forces, for example, the gravitational constant $g$, or the density of electric or magnetic forces, while the fractal material time derivative is defined by Eq. (47). Using the continuity equation (49), the balance of density of momentum in fractal continuum can be presented in the following form:

$$\left(\frac{d}{dt}\right)_D u_i = \frac{\partial}{\partial t}u_i + u_i\nabla_j^H u_j = f_i + \rho_c^{-1}\left(\nabla_i^H p + \nabla_j^H \sigma_{ij}^v\right), \tag{55}$$

which converts into the conventional equation of the density of momentum balance when $d_i = D - 1$ for all $i$. Notice that Eq. (55), together with the mass conservation equation (49) and appropriate boundary conditions, are sufficient to describe the steady flow of an inviscid ($\sigma_{ij}^v \equiv 0$) incompressible ($\rho_c =$ const) fractal continuum.

The internal energy $dE$ of an element of fractal continuum of the mass $dM_D$ is equal to $dE = e(x_i,t)\rho_c(x_i,t)dV_D$, where $e(x_i,t)$ is the internal energy density, while the kinetic energy of the mass $dM_D$ moving with the velocity $\vec{u}(x_i t)$ is equal to $dT = 0.5\rho_c|\vec{u}|^2$. Accordingly, the total energy of region $W$ of fractal continuum is defined as follows:

$$U = E + T = \int_W \rho_c\left(e + \frac{u^2}{2}\right)dV_D.$$

The change of the total energy of region $W$ can be defined as

$$U(t_1) - U(t_2) = \Omega_M + \Omega_S + Q_S,$$

where $\Omega_M$ is the work of mass forces $\vec{f}\rho_c dV_D$, $\Omega_S$ is the work of surface forces $\sigma_{ij}n_i\vec{e}_i dV_D$, $\sigma_{ij}$ is the Cauchy stress tensor, and $\vec{Q}_S = \rho_c\vec{\gamma}$ is the heat that are influx into the region $W \in {}^D_{d_\ell}\Phi^3_D \subset E^3$ through the surface $\partial W$, while $\vec{\gamma} = \gamma_i n_i$ is the heat influx density. Therefore, the rate of the total energy change can be presented as follows:

$$\frac{d}{dt}\int_W \rho_c\left(e + \frac{u^2}{2}\right)dV_D = \int_W \rho_c u_i f_i dV_D + \int_{\partial W}\left(u_i\sigma_{ij}n_i e_i + n_i\gamma_i\right)dA_d. \tag{56}$$

Employing the generalized Green-Gauss divergence theorem (33), Eq. (56) can be rewritten in the following form:

$$\int_W \left[\rho_c\left(\frac{d}{dt}\right)_D e - \sigma_{ij}\nabla_j^H u_i - \rho_c\nabla_i^H\gamma_i\right]dV_D, \tag{57}$$

which is valid for any region $W$ of the fractal continuum ${}^D_{d_\ell}\Phi^3_D \subset E^3$, while the material time derivative is defined by Eq. (47). Hence, the differential equation of energy density balance in the fractal continuum flow has the following form:

$$\rho_c\left(\frac{d}{dt}\right)_D e = \rho_c\frac{\partial e}{\partial t} + u_i\rho_c\nabla_i^H e = \sigma_{ij}\nabla_j^H u_i + \rho_c\nabla_i^H\gamma_i. \tag{58}$$

Notice that Eq. (58) converts into the conventional equation of energy density balance when any intersection of the continuum flow with Cartesian planes is characterized by the same fractal dimension (7).

Here, it is pertinent to note that in the case of an anomalous diffusion of fractal continuum with the intrinsic time scale dimension $\alpha_\tau < 1$, the continuity equation has the following form:

$$\nabla_t^H\rho_c = -\mathrm{div}_H(\rho_c\vec{v}). \tag{59}$$

Taking into account the definitions of Hausdorff partial time derivative (35) and particle velocity (41), Eq. (59) can be rewritten in the form of Eq. (49) with the flow velocity defined as

$$\vec{u} = \frac{\partial}{\partial t}\vec{v} = \left(\frac{t}{\tau_0} + 1\right)^{\alpha_t - 1}\vec{v}.$$

At the same time, the equation for balance of density of momentum in the case anomalous diffusion of fractal continuum can be presented in the form

$$\begin{aligned}\left(\frac{d}{d^H t}\right)_D v_i &= \nabla_t^H v_i + v_i\nabla_j^H v_j \\ &= \chi_\tau^2\left(\frac{\partial u_i}{\partial t} + \frac{u_i}{t+\tau_0} + u_i\nabla_j^H u_j\right) \\ &= f_i + \rho_c^{-1}\left(\nabla_i^H p + \nabla_j^H\sigma_{ij}^v\right).\end{aligned} \tag{60}$$

Equation (60) implies that the momentum cannot be conserved during an anomalous diffusion of fractal continuum. Furthermore, it should be pointed out that the failure of the momentum conservation law is the common feature of phenomenological models of fractal flow based on the concept of anomalous diffusion.

### E. Gravitational head and hydrostatic pressure distributions in fractal continuum

When a fractal continuum is at rest and the volume force field is determined by gravitation only, Eq. (55) of momentum density balance in fractal continuum reduces to the condition for hydrostatic equilibrium in the fractal continuum

$$\mathrm{grad}_H p = \rho\vec{g}, \tag{61}$$

where vector $\mathrm{grad}_H p$ defined by Eq. (26) expresses the magnitude and direction of the maximum spatial rate of increase of the scalar property $p$. It should be emphasized that hydrostatic distribution (61) is valid for any fractal continuum at rest, regardless of its viscosity, because the viscous term vanishes identically. In the hydrostatic condition, the pressure variation is due only to the weight of the fluid. Notice that the maximum pressure increase will be in the direction of the gravity field.

In a given gravity field, the pressure may easily be calculated by integration of Eq. (61). If fractal continuum is so nearly incompressible that we can neglect their density variation in the hydrostatic equilibrium, the pressure distribution in a homogeneous fractal continuum has the form

$$p(z) = p_0 - g(D - d_z)\rho_0\ell_z\left(\frac{z}{\ell_z} + 1\right)^{D-d_z}, \tag{62}$$

where $p_0 = p(z = 0)$ is the pressure on the free surface normal to the gravitational field. Notice that when $D - d_z < 1$, the gravitational head increases with the fluid elevation more

slowly than in the Euclidean case and when the equality (7) holds.

### F. Generalized Euler equation and Bernoulli integral

For inviscid fractal continuum flow in a gravitational field, Eq. (55) reduces to the generalized Euler equation in the form

$$\rho_c \left(\frac{d}{dt}\right)_D \vec{u} = \rho_c \vec{g} - \mathrm{grad}_H\, p, \tag{63}$$

which resembles the classic form of Euler equation and converts to it when the equality (7) holds. From Eq. (63) immediately follows that the generalization of Bernoulli integral for a steady incompressible flow of inviscid fractal continuum in the gravitational field can be represented as

$$\sum_k^3 \frac{u_k^2}{2} + \frac{p}{\rho_0} + g(D-d_z)\ell_z \left(\frac{z}{\ell_z}+1\right)^{D-d_z} = h = \mathrm{const}, \tag{64}$$

where the notations $z = x_3$, $\ell_z = \ell_3$, and $d_z = d_3$ are used, while $h$ is the total hydraulic head. It is important to note that Eq. (64) can be relatively easily verified in laboratory experiments with prefractal porous reservoirs (see Ref. [8]). Notice that, generally, the total hydraulic head can be presented as the sum of elevation, pressure, fluid velocity, osmotic, and other potentials.

### G. Sound waves in fractal continuum flow

The wave equation in a fractal continuum can be derived by considering small perturbations to the governing balance laws describing the dynamics of the fractal continuum flow. In the case of isotropic fractal continuum flow the isentropic (adiabatic and reversible) oscillations of pressure, density, and flow velocity about an equilibrium point $(p_0, \rho_0, \vec{u}_0 = 0)$ can be presented as

$$p = p_0 + p', \quad \rho_c = \rho_0 + \rho', \quad \text{and} \quad u_i = u_i^{(0)} + u_i', \tag{65}$$

respectively, where $p' \ll p_0$, $\rho' \ll \rho_0$, and $u_i' \ll u_i^{(0)}$, while

$$\frac{\partial p_0}{\partial t} = 0, \quad \frac{\partial p_0}{\partial x_i} = 0, \quad \frac{\partial \rho_0}{\partial t} = 0, \quad \frac{\partial \rho_0}{\partial x_i} = 0. \tag{66}$$

Substituting (65), in Eqs. (49) and (55) under condition $f_i = 0$, we obtain the following equations for the first order of the perturbation:

$$\frac{\partial \rho'}{\partial t} = -\rho_0 \nabla_i^H u_i' \quad \text{and} \quad \frac{\partial u_i'}{\partial t} = -\rho_0^{-1} \nabla_i^H p'. \tag{67}$$

Taking the partial time derivative of the first equation of Eq. (67) and substituting the result into the second equation of Eq. (67) we get

$$\frac{\partial^2 \rho'}{\partial t^2} = \nabla_i^H \nabla_i^H p'. \tag{68}$$

For adiabatic process $p = p(\rho_c, S)$ and so, for the first order of perturbation we have

$$p' = a^2 \rho', \quad \text{where} \quad a = \sqrt{\left(\frac{\partial p}{\partial \rho}\right)_S} \tag{69}$$

is the sound velocity. Accordingly, the wave equations in an isotropic fractal continuum flow can be written in the following form:

$$\frac{\partial^2 \rho'}{\partial t^2} = a^2 \Delta_H \rho' \quad \text{and} \quad \frac{\partial^2 p'}{\partial t^2} = a^2 \Delta_H p', \tag{70}$$

where the Hausdorff Laplacian is defined by Eq. (24). Notice the difference between Eq. (70) and the wave equation derived in Ref. [29]. It is easy to see that the wave equations (70) can be converted in the conventional equations for sound propagation in a fluid by the change of variables $x_i \to x_i/\chi^{(i)}$. Consequently, the solutions of Eqs. (70) can be easily obtained by the change of variables in the corresponding solutions of the conventional wave equations in fluids.

### H. Fractal continuum hydrodynamics

To develop fractal continuum hydrodynamics we need to use two fundamental types of laws: the conservation laws and the constitutive laws. The above-derived conservation laws describe the conservation of matter, energy, and momentum, while the constitutive law should define the relationship between the displacements in the fractal continuum and the applied forces. The constitutive laws of continuum mechanics cannot be deduced from the laws of mechanics of material points and rigid bodies, but can be defined from physical experiments, for example, Hooke's law of elasticity, the Newtonian viscosity law, etc. To derive the hydrodynamic equations for fractal continuum flow, the constitutive relations of classical hydrodynamics should be mapped into the fractal continuum framework. In this way, there are a number of rules that must be used to produce constitutive equations that are admissible from the rational and physical standpoints. Specifically, the constitutive equations should be invariant under any change of reference frame. Furthermore, the current rheological and thermodynamic state of the material should be completely determined by the history of the thermokinetic process experienced by the material. Specifically, in the case of incompressible materials, the stress state is determined to within the hydrostatic pressure, which depends on the boundary conditions and the problem geometry. Besides, the stress tensor at a given point does not depend on movements occurring at finite distance from this point.

Experimental observations suggest that when a fluid is sheared, it begins to move at a strain rate inversely proportional to fluid viscosity [36]. In the case of the Euclidean flow of a Newtonian fluid, such as water and oils, the strain rate is a linear function of applied shear. The Stokes constitutive law for Euclidean continuum flow of a Newtonian fluid has the following form:

$$\sigma_{ij} = -p\delta_{ij} + \mu\left(\frac{\partial u_j}{\partial x_i} + \frac{\partial u_i}{\partial x_j} - \frac{2}{3}\frac{\partial u_l}{\partial x_l}\right) + \lambda \frac{\partial u_l}{\partial x_l}\delta_{ij}, \tag{71}$$

where $p$ is the fluid pressure, $\mu$ is the dynamic viscosity, $\lambda$ is the coefficient of internal viscosity, and $\delta_{ij}$ is the Kronecker's $\delta$ [37]. Notice that the viscosity of Newtonian fluids is a true thermodynamic property which varies with temperature and pressure [36]. In the case of fractal continuum flow, the definition of fractal Jacobian (39) implies that the tensor of stresses in compressible Newtonian fluid should be presented

in the following form:

$$\sigma_{ij} = -p\delta_{ij} + \mu\left(\nabla_i^H u_j + \nabla_j^H u_i - \tfrac{2}{3}\nabla_l^H u_l\right) + \lambda\nabla_l^H u_l \delta_{ij}, \tag{72}$$

which expresses the linear relation between the shear stresses and the pure shear strain rates in the fractal continuum ${}_3^D\Phi_D^3 \subset E^3$, whereas the conventional form of constitutive equation (71) in the case of fractal continuum flow implies a nonlinear dependence between the shear stresses and the pure shear strain rates in the fractal continuum.

Substituting Eq. (72) into Eq. (55) and making use the vector fractional differential operators, we get the generalized Navier-Stokes equation for fractal continuum flow ${}_3^D\Phi_D^3 \subset E^3$ in the vector form,

$$\rho_c\left[\frac{\partial\vec{u}}{\partial t} + (\vec{u}\cdot\nabla^H)\vec{u}\right] = -\mathrm{grad}_H\, p + \mu\Delta_H\vec{u} + \left(\lambda + \frac{\mu}{3}\right)\mathrm{grad}_H \mathrm{div}_H\vec{u} + \vec{f}, \tag{73}$$

which resembles the vector form of the classic Navier-Stokes equations describing the motion of a Newtonian fluid in $E^3$. Notice that Eq. (73) converts into the classic Navier-Stokes form if $d_i = D - 1$ for any intersection of fractal continuum flow with a two-dimensional plane in $E^3$ [38].

In the case of generalized fractal continuum flow ${}_{d_\ell}^D\Phi_D^3 \subset E^3$ with a nontrivial topology characterized by $d_\ell < 3$, the generalized Newtonian constitutive equation can be different from Eq. (73). While we cannot define the general constitutive equation for fractal continuum flow ${}_{d_\ell}^D\Phi_D^3 \subset E^3$ in the form of generalized Stokes law, in the next section, the fractal topology of fractal continuum flow ${}_{d_\ell}^D\Phi_D^3 \subset E^3$ will be accounted for in the phenomenological form of the pressure-transient equation for the generalized fractal continuum flow.

## IV. MAPPING OF FLUID FLOW IN FRACTALLY PERMEABLE MEDIUM INTO FRACTAL CONTINUUM FLOW

Fluid transport in porous media can be described on two fundamental scales: the microscopic pore scale and the Darcy scale [1]. On the pore scale, transport phenomena are governed by the classic Navier-Stokes and advection-diffusion equations, whereas on the Darcy scale, the fractal flow is expected to obey the fractal continuum hydrodynamics. In fact, the question of whether a fluid flow in porous medium can be considered as a continuum flow for the solution of specific problems or analysis of some experimental data is often a subjective matter. The concept of a continuum is an idealization, which may approximate reality when one looks at the appropriate distance and time averages. Therefore, the term "continuous" commonly means that various properties averaged on a length and time scale of interest vary smoothly within the region except possibly for a small number of discontinuities. Accordingly, heterogeneous media are often modeled in a continuum framework using an effective medium or mean field approaches (see, for example, Refs. [39,40]). In this context, the fractal continuum hydrodynamics can provide an overall description of fluids flow in a fractal porous medium.

Consequently, fluid flow in a fractally permeable medium should be mapped into the flow of the three-dimensional fractal continuum ${}_{d_\ell}^D\Phi_D^3 \subset E^3$ with the fractal quasimetrics defined by a nonuniform distribution of the degrees of freedom for its points (see Fig. 1). The simplest case of fractal flow in permeable media is flow of a single homogenous fluid phase through a porous and/or fissured solid. The mapping of fluid flow in a fractally permeable medium into the fractal continuum flow implies that the density of the fractal continuum $\rho_c$ is related to the fluid density $\rho_f$ as

$$\rho_c = \phi\rho_f, \tag{74}$$

where $\phi$ is the effective porosity of the fractally permeable medium. Consequently, the dynamic viscosity of fractal continuum flow is related to the fluid's dynamic viscosity $\mu_f = \rho_f\eta_f$ as

$$\mu_c = \eta_c\rho_c = \eta\phi\rho_f = \phi\mu_f, \tag{75}$$

while the kinematic viscosity of fractal continuum $\eta_c$ is assumed to be equal to the fluid's kinematic viscosity, that is, $\eta_c = \eta_f = \eta$ (see Table III).

Furthermore, in this work we assume that the fractal continuum flow ${}_{d_\ell}^D\Phi_D^3 \subset E^3$ is governed by the balance equations (49), (55), and (58) associated with the fractal metric defined by Eqs. (8)–(13), while the form constitutive equation depends on the fractal flow topology characterized by the chemical dimension $d_\ell$, whereas the spectral dimension of hydrodynamic (Darcian) flow is always $d_s = D$, even when the spectral dimension of fractally permeable porous medium is less than its mass fractal dimension (see Table II and discussion in Sec. III A). Formally, the equality $d_s = D$ can be interpreted as a consequence of equality $D_W^{\mathrm{Darcian}} = 2$ under the assumption that the fractal continuum flow obeys the Alexander-Orbach law [41] $d_s = 2D/D_W = 2D/(2+\theta)$ (see Ref. [11]). In fact, however, the Alexander-Orbach law is intimately linked to a specific form of the fractal Einstein law related the electrical resistivity exponent $\vartheta$ to the fractal dimensions of medium and random walk [42]. It was proved that the Alexander-Orbach law holds if $\vartheta = D_W - D > 0$ [43], but otherwise it can be failed [44]. In the last case, the fractal Einstein law has a more general form $\vartheta = 0.5D_W(2 - d_s)$, where $D_W$ and $d_s$ are independent characteristics of the corresponding fractal structure [44]. Hence, the random walk in the fractal continuum flow can have the fractal dimension $D_W \neq 2$, even if $d_s = D$. The knowledge of the fractal dimension of random walk in the fractal continuum flow is important in modeling the diffusion in the flow (see Table II).

In this work, we are especially interested in either the stationary flow through a porous and/or fissured medium, conventionally described by Darcy's law (see Refs. [1]), or the pressure transients in porous (fissured) reservoirs, commonly described using the equations derived by the substitution of Darcy's law into the continuity equation (see Refs. [45,46]). Both cases are discussed below.

### A. Analog of Darcy's law for fractal continuum flow

Historically, Darcy's law was introduced in a phenomenological way for single-phase flow through sand. In its original form Darcy's law states that the flux $Q$ of a single phase fluid

TABLE III. Relations between the properties of fractal continuum flow, the properties of the fractally permeable medium, fluid, and the flow dynamics and geometry.

| | Flow in porous and/or fissured medium | | | |
|---|---|---|---|---|
| Parameter | Permeable medium | Fluid | Fluid flow | Fractal continuum flow |
| Porosity | $\phi$ | | | |
| Characteristic size $\ell_0$ | Eq. (2) | | | Eqs. (1) and (12) |
| Tensor of absolute permeability | $K_{ij}$ | | | |
| Relative permeability | | | $k_{ij}$ | |
| Effective property of continuum flow related to the medium permeability | | | | $K_{ij}^{(c)} = f(K_{ij},k_{ij})$ |
| Fractal properties | See Table I | | Determined by the fractal geometry of permeable medium | See Table II |
| Flow dimension | | | See Fig. 3 | $d_\ell$ |
| Density | $\rho_m = \rho_0(1-\phi)$ | $\rho_f$ | $\rho_f(p,x_i,t)$ | Eq. (74) |
| Compressibility | $c_m$ | $c_f$ | Eq. (85) | Eqs. (90) and (91) |
| Constitutive law | | Newtonian | Eq. (71) | Eq. (72) |
| Kinematic viscosity | | | $\eta_f = \eta$ | $\eta_c = \eta$ |
| Dynamics viscosity | | | $\mu_f = \rho_f \eta$ | Eq. (75) |
| Coefficient of internal viscosity | | | $\lambda_f$ | $\lambda_c = \phi\lambda_f$ |
| Flow velocity ($u$) | | | Eq. (45) | Eqs. (45) and (52) |
| Darcian velocity | | | Eq. (77) | Eq. (80) |
| Hydrostatic head | | | $gz(x,y)$ | Eq. (62) |

is related to the pressure drop $\Delta p$ over sample length $L$ as

$$Q = A_2 \frac{K}{\mu} \frac{\Delta p}{L}, \tag{76}$$

where $A_2$ is the area of cross section and $K$ is the intrinsic permeability of the porous medium [36]. Accordingly, the Darcy velocity, defined as

$$q = Q/A_2 = \phi u, \tag{77}$$

is not a true velocity of the fluid, but represents an effective flow rate through the porous medium. Strictly speaking, Darcy's law holds only for Newtonian fluids over a certain range of flow rates. As the flow rate increases, the deviations from this law have been noticed. It has been experimentally observed and mathematically shown that these deviations are due to inertia, turbulence, and other high-velocity effects (see Refs. [47] and references therein).

Although Darcy's law was proposed from empirical arguments, Hubbert [48] showed that an equation similar to Darcy's law can be obtained from averaging equations of flow for fluids on the microscale. Further, in Ref. [49] it was showed that Darcy's law may actually result from the macroscale momentum balance equation by upscaling of pore-scale mass, momentum, energy, and entropy balances in the framework of a thermodynamic averaging theory and applying a large set of assumptions. Afterward, the authors of [50] have developed a more rigorous approach that includes the use of spatial averaging theorems to obtain the expression of Darcy's law for three-dimensional flow in the following form:

$$\vec{q} = -\frac{K_{ij}}{\mu}(\nabla p - \rho \vec{g}), \tag{78}$$

where the intrinsic permeability tensor $K_{ij}$ is assumed to be a property of the porous medium and $\vec{g}$ is the gravity vector. The same relationship between pressure gradient and flow rate has been found by rigorously homogenizing the Navier-Stokes equations but imposing the assumptions that inertial forces and friction within the fluid can be neglected [51].

The effect of fractal geometry of porous media on the Darcian flow was discussed in Refs. [52]. In these works a convolved version of Darcy's law based on a fractional integral was proposed. The generalized Darcy law employing the Riemann-Liouville fractional derivative was suggested in Ref. [53]. In Ref. [54] Darcy's law was modified, introducing general memory formalisms operating on the flow as well as on the pressure gradient, which imply a filtering of the pressure gradient without singularities. In this context, the authors of [55] have proposed fractional geometry to model and explain deviations of Darcy's velocity due to fractured rocks in aquifers. Further, based on the study by O'Shaugnessy and Procaccia [56] on anomalous fractal diffusion, the authors of [57] have suggested that the permeability of fractal fracture network vary as a power of distance from the source term $r$, that is,

$$K_r \propto r^{D_n - D_E - \theta}, \tag{79}$$

where $D_E$ and $D_n$ are the Euclidean and fractal dimensions of fracture network, respectively, while $\theta \geqslant 0$ is the anomalous diffusion exponent related to the dimension of random walk as $\theta = D_W - 2$. The classical Darcy's law was generalized by regarding fluid flow as a function of a noninteger order spatial derivative of the piezometric head [58]. More recently, a fractional-order Darcy's law was derived from a fractional Newton's law of viscosity employing nonlocal fractional calculus [59].

A rigorous derivation of the generalized Darcy's law for a fractal continuum flow from the generalized Navier-Stokes equation (73) represents a challenging task for further research. The specific expression related the hydraulic head and flow

velocity is dependent on the assumptions used to perform the averages in the fractal continuum flow ${}^{D}_{d_\ell}\Phi^3_D \subset E^3$. Even though, following the Darcy's law derivation in Ref. [60], but employing fractional Hausdorff operators (24)–(28), here we anticipate that the generalized Darcy's law for fractal continuum flow ${}^{D}_{3}\Phi^3_D \subset E^3$can be expressed in the following form:

$$u_i = -\frac{K^{(c)}_{ij}}{\mu_c}\nabla^H_i(p - h_g), \tag{80}$$

where the pressure $p(x_i)$ and the gravitational head $h_g(x_i)$ are, generally, functions of Cartesian coordinates $x_i \in E^3$, while $K^{(c)}_{ij}$ is the characteristic tensor property of the fractal continuum flow associated with the permeability tensor $K_{ij}$ in the fractally permeable medium under consideration (see Table III). Notice that for reservoirs and wells of known geometry the gravitational head can be defined in a usual way taking into account Eq. (62), while $\mathrm{div}_H \vec{u} = \psi(x_i)$, wherein $\psi(x_i)$ is the source/sink term.

It is interesting to note that Eq. (80) resembles the classic Darcy's law (78) with the spatially varying permeability (79) regardless the expression for the permeability scaling exponent. In fact, assuming that $K^{(c)}_{ii} = K_i$, while in the principal coordinates $K^{(c)}_{ij} = 0$, and taking into account relationship (75), Eq. (80) can be rewritten in the form of Eq. (78) as

$$\vec{q} = \phi\vec{u} = -\frac{K^A_i}{\mu_f}\mathrm{grad}(p - h_g), \tag{81}$$

with the spatially varying apparent permeability

$$K^A_i \propto \chi^{(i)}K_i \propto x_i^{1-D+d_i}. \tag{82}$$

Furthermore, in terms of the Darcy experiment, Eqs. (81) and (82) can be presented in the form

$$Q = A_d\frac{K\ell_0^{D-d_L-1}}{\mu}\frac{\Delta p}{L^{D-d_L}}, \tag{83}$$

which can be used for the experimental validation of the generalized Darcy's law (80). If we chose $A_2 \propto L^2$, Eq. (83) implies that the apparent permeability scales with the reservoir size $R$ as

$$K^A \propto R^{2d-1-D}, \tag{84}$$

because $A_d \propto L^{d-2}$, while $q = Q/A_2$. Notice that the power-law increase of hydraulic conductivity with increasing scale of measurement is consistent with the field observations from many sources (see Refs. [61]).

It is important to point out that, regardless of the similarity of Eq. (80) to Darcy's law (78) with the spatially varying permeability (79), the physical essences of these models are different. In fact, the power-law scaling of fractal permeability (79) accounts for the fractal geometry of porosity ($\phi \propto r^{D-D_E}$) and the anomalous diffusion characterized by the diffusion coefficient $D_{\mathrm{dif}} \propto r^{-\theta}$, whereas the power-law scaling of apparent permeability (81) reflects the metric properties of the fractal continuum, while an anomalous diffusion plays no role in the case of Darcian flow of a fractal continuum (see Table II).

### B. Pressure-transient equations for fractal continuum flow

Mathematical models of petroleum reservoirs have been utilized since the late 1800s. The major goal of reservoir simulation is to predict future performance of the reservoir and find ways and means of optimizing the recovery of some of the hydrocarbons under various operating conditions. A mathematical model consists of a set of equations that describe the flow of fluids in a petroleum reservoir, together with an appropriate set of boundary and/or initial conditions [45]. A standard method to characterize hydraulic properties of porous and/or fissured media is the pressure-transient analysis of pumping test data. Pressure-transient testing techniques, such as pressure drawdown, buildup, injection, fallow, and interference tests are widely used to analyze and forecast reservoir performance [46]. During a well test, the response of a reservoir to changing production (or injection) conditions is monitored. Since this response is related to reservoir properties, it is possible in many cases to infer reservoir properties from the response. Therefore, the well test interpretation is an inverse problem in which model parameters are inferred by analyzing model response to a given input.

During a well test, a transient pressure response is created by a temporary change in production rate. In most cases, the flow rate is measured at the surface while the pressure is recorded downhole. Before opening, the initial pressure $p_0$ is assumed to be constant and uniform in the reservoir. During the flowing period, the drawdown pressure response is defined as the pressure drop $\Delta p = p_0 - p(x_i,t)$. When the well is shut-in, the buildup pressure change $\Delta p = p(t) - p_*$ is estimated from the last flowing pressure $p_* = p(\Delta t = 0)$. The pressure response is analyzed versus the elapsed time $\Delta t$ since the start of the period (time of opening or shut-in). In practice, for a given period of the test, the change in pressure $\Delta p$ is plotted on log-log scales versus the elapsed time $\Delta t$, while the test period is defined as a period of constant flowing conditions, for example, constant flow rate for a drawdown or shut-in period for the buildup test (see Refs. [45]).

Conventional pressure-transient models have been developed under the assumption of a homogeneous reservoir. Accordingly, to describe the pressure transient in a porous reservoir, the Darcy equation (78) is combined with the equation of continuity and an equation of state for fluid under consideration. In the case of a slightly compressible fluid, it is assumed that $\partial\rho_f/\partial p = c_f\rho_f$, where $c_f$ is the coefficient of fluid compressibility. If a porous medium is also slightly compressible, the time derivative of fluid density can be replaced by

$$\frac{\partial\rho_f}{\partial t} = c\rho_f\frac{\partial p}{\partial t}, \tag{85}$$

where $c = c_f + c_m$ is the system compressibility, while $c_m$ is the coefficient of matrix compressibility [46]. Accordingly, the pressure transient in an isotropic radial flow obeys the following diffusion equation:

$$c\mu\phi\frac{\partial p}{\partial t} = \frac{K_r}{r^{n-1}}\frac{\partial}{\partial r}\left(r^{n-1}\frac{\partial p}{\partial r}\right), \tag{86}$$

where the flow dimension $n$ reflects how the apparent flow area changes with distance from the source (see Fig. 3) and is not necessarily related to the space filling nature of the flow, in the

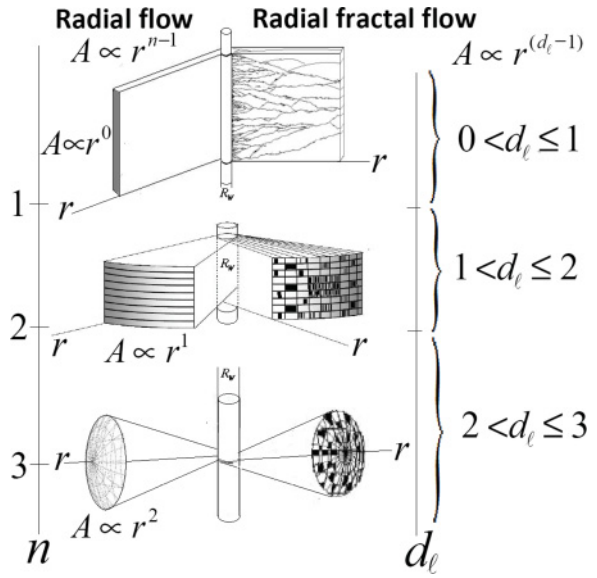


FIG. 3. The definition of flow dimensions $n$ and $d_\ell$ in the case of radial flow in a fractally permeable medium.

sense that the apparent surface area of one-dimensional flow is constant regardless of the distance from the well, whereas the surface area of two-dimensional flow is proportional to $r^1$ and that of three-dimensional flow is proportional to $r^2$. Therefore, in the case of one-dimensional flow $n = 1$, while in the case of radial flow in cylindrical geometry $n = 2$, and $n = 3$ in the case of spherical symmetry of radial flow. In practice (see Refs. [45,46]), the data of well tests are commonly fitted using the dimensionless variables defined in Table IV.

Although pressure-transient equation (86) and its analogs in the Cartesian coordinates are sometimes used in petroleum engineering, today it is widely accepted that in many cases the experimental field data could not be satisfactorily described using Euclidean models of natural reservoirs. This stimulates the use of fractal geometry for reservoir modeling. In this context, Barker [62] has proposed a pressure-transient equation involving the fractional dimension of flow, while retaining the assumptions of radial flow and homogeneity of the fractured medium. The celebrated Barker equation can be written in the following dimensionless form:

$$\frac{\partial p_D}{\partial t_D} = \frac{1}{r_D^{D^*-1}} \frac{\partial}{\partial r_D} \left( r_D^{D^*-1} \frac{\partial p_D}{\partial r_D} \right) = \frac{\partial^2 p_D}{\partial r_D^2} + \frac{D^* - 1}{r_D} \frac{\partial p_D}{\partial r_D}, \tag{87}$$

where $0 < D^* \leqslant 3$ is the flow dimension which can be assumed to be fractional (see Fig. 3) and the dimensionless variables are defined in Table IV. It should be pointed out that Barker [58] considered the physical meaning of the flow dimension unclear, but conjectured that it would be related to the anomalous diffusion on fractal fracture network. Still, the Barker pressure-transient equation has become very popular, especially for practical applications (see Refs. [63] and references therein).

Although, originally, Eq. (87) was derived using a geometric model of fractured reservoir, we noted that it can be obtained from Eq. (86) by the substitution of the Laplacian on $n$-dimensional Euclidean sphere with the fractional Laplacian (16). In this framework, Eq. (87) can be generalized for anisotropic reservoirs as

$$\frac{\partial p_D}{\partial t_D} = \nabla_D^2 p_D = \sum_i^3 \left( \frac{\partial^2 p_D}{\partial x_{Di}} + \frac{\alpha_i - 1}{x_{Di}} \frac{\partial p_D}{\partial x_{Di}} \right), \tag{88}$$

using expression (17) for the fractional Laplacian in the dimensionless Cartesian coordinates $x_{Di}$. Notice that the fractional Laplacian (17) introduced in Refs. [26,27] is related to the flow topology characterized by the chemical dimension (23).

On the other hand, assuming the spatial variation of hydraulic permeability according to relation (78), Chang and Yortsos [57] have suggested the equation of radial fractal flow which in the dimensionless form reads as

$$\begin{aligned} \frac{\partial p_D}{\partial t_D} &= \frac{1}{r_D^{D_n-1}} \frac{\partial}{\partial r} \left( r_D^{D_n-1-\theta} \frac{\partial p_D}{\partial r_D} \right) \\ &= \frac{1}{r_D^{\theta}} \left( \frac{\partial^2 p}{\partial r_D^2} + \frac{D_n - 1 - \theta}{r_D} \frac{\partial p_D}{\partial r_D} \right), \end{aligned} \tag{89}$$

where $D_n$ is the fractal (mass) dimension of fracture network, while the dimensionless variables are defined in Table IV. Notice that in the case $\theta = 0$, Eq. (89) converts into Eq. (87),

TABLE IV. Dimensionless variables for the pressure-transient equations at a constant production rate. Here $r_D$ is the dimensionless radial distance from the pumping well, $t_D$ is the dimensionless time, $p_D$ is the dimensionless pressure drop, $p_0$ is the initial pressure, $R_W$ is the well radius, $Q$ is the volumetric flow rate, and the coefficients $\kappa_n$ are defined as follows: $\kappa_1 = HR_W, \kappa_2 = 2\pi H, \kappa_3 = 4\pi$, while $\kappa_n^D = 2^{D^*-1}\pi R_W^{3-D^*}$ and $\kappa_n^\theta = R_W^{3-D_n+\theta}$.

| Model and pressure-transient equation | Dimensionless variables | | |
|---|---|---|---|
| | $t_D = t/\tau_c$ | $p_D = (p_0 - p)/p_c$ | $r_D = r/r_c$ |
| Euclidean, Eq. (86) | $\tau_c = \frac{c\mu\phi R_W^2}{K_r}$ | $p_c = \frac{Q\mu}{\kappa_n R_W^{n-2} K_r}$ | $r_c = R_W$ |
| Barker, Eq. (87) | $\tau_c = \frac{c\mu\phi R_W^2}{K_r}$ | $p_c = \frac{Q\mu}{\kappa_n^D R_W^{D^*-2} K_r}$ | $r_c = R_W$ |
| Chang and Yortsos, Eq. (89) | $\tau_c = \frac{c\mu\phi R_W^{2+\theta}}{K_r}$ | $p_c = \frac{Q\mu}{\kappa_n^\theta R_W^{D_n-\theta-2} K_r}$ | $r_c = R_W$ |
| ${}_3^D\Phi_D^3$, Eq. (94) | $\tau_c = \frac{c\mu\phi r_c^2}{K_r}$ | $p_c = \frac{Q\mu}{\kappa_n r_c^{n-2} K_r}$ | $r_c = \frac{R_W}{2^{\zeta-1}} \left( \frac{R_W}{\ell_0} + 1 \right)^{\zeta-1}$ |
| ${}_{d_\ell}^D\Phi_D^3$, Eq. (97) | $\tau_c = \frac{c\mu\phi r_c^2}{K_r}$ | $p_c = \frac{Q\mu}{4\pi r_c K_r}$ | $r_c = \frac{R_W}{2^{\zeta-1}} \left( \frac{R_W}{\ell_0} + 1 \right)^{\zeta-1}$ |

even though these equations are derived using two completely different geometrical approaches. However, in contrast to Eqs. (87) and (89) cannot be directly generalized for an anisotropic three-dimensional flow with spatially varying permeability.

To derive the transient pressure equation for a fractal continuum flow ${}^{D}_{3}\Phi^{3}_{D} \subset E^{3}$, we note that in the case of a slightly compressible fractal continuum $\partial\rho_c/\partial p = c\rho_c$ and so

$$\frac{\partial \rho_c}{\partial t} = c\rho_c \frac{\partial p}{\partial t}, \tag{90}$$

as is usually assumed in the hydrodynamics of slightly compressible liquids [see Eq. (85)], while the coefficient of fractal continuum compressibility $c$ is determined by the fluid compressibility $c_f = \partial \ln \rho_f/\partial p$ and the compressibility of porous medium $c_\phi = \partial\phi/\partial p$ as

$$c = c_f + \phi c_\phi. \tag{91}$$

Substituting Eqs. (80) and (90) into Eq. (49) we obtain the following equation of pressure diffusion in an anisotropic three-dimensional fractal continuum flow,

$$\begin{aligned} c\mu_c \frac{\partial p}{\partial t} &= \mathrm{div}_H\left[K^{(c)}_{ii}\mathrm{grad}_H(p-h_g)\right] \\ &= \sum_i^3 K^{(c)}_{ii}\left(\frac{x_i}{\ell_i}+1\right)^{2(1+d_i-D)}\left[\left(\frac{\partial^2(p-h_g)}{\partial x_i^2}\right)\right. \\ &\quad \left. + \frac{1+d_i-D}{x_i+\ell_i}\left(\frac{\partial(p-h_g)}{\partial x_i}\right)\right], \end{aligned} \tag{92}$$

where $h_g$ is the gravitational head defined by Eq. (62).

For reservoirs and wells of known geometry Eq. (92) together with appropriate inner and outer boundary and initial conditions can be used to model the pressure transients of fractal flow. Notice that in the case of Euclidean porosity, as well as in the case of isotropic fractal porosity ($K^{(0)}_{ij} \equiv K_0$) obeying Mandelbrot's rule of thumb (7), Eq. (92) converts into the classical pressure-transients equation

$$c\mu_f\phi\frac{\partial p}{\partial t} = K_0\Delta(p-h_g), \tag{93}$$

which in the case of radial isotropic flow ($h_g = 0$) through a $n$-dimensional sphere (see Fig. 3) takes the form of Eq. (86).

Furthermore, from (92) immediately follows that the radial flow of an isotropic fractal continuum through a $d_r$-dimensional intersection of fractal continuum with $n$-dimensional sphere obeys the following pressure-transient equation:

$$\begin{aligned} \frac{\partial p_D}{\partial t_D} &= \frac{\chi^{(r)}_D}{(r_D+\ell_D)^{n-1}}\frac{\partial}{\partial r_D}\left[(r_D+\ell_D)^{n-1}\chi^{(r)}_D\frac{\partial}{\partial r_D}p_D\right] \\ &= \left(\frac{r_D}{\ell_D}+1\right)^{d_r+2-D-n}\frac{\partial}{\partial r_D}\left[\left(\frac{r_D}{\ell_D}+1\right)^{d_r-D+n}\frac{\partial}{\partial r_D}p_D\right] \\ &= \left(\frac{r_D}{\ell_D}+1\right)^{2(d_r+1-D)}\left(\frac{\partial^2 p_D}{\partial r_D^2}+\frac{d_r+n-D}{r_D+\ell_D}\frac{\partial p_D}{\partial r_D}\right), \end{aligned} \tag{94}$$

where the dimensionless variables are defined in Table IV, while the integer exponent $n$ is determined by the flow symmetry: $n = 1$ in the case of one-dimensional flow, $n = 2$ in the case of radial flow in cylindrical geometry, and $n = 3$ in the case of spherical radial flow (see Fig. 3), while

$$\chi^{(r)}_n = \left(\frac{r_D}{\ell_D}+1\right)^{d_r+1-D}, \tag{95}$$

in all cases [$\ell_D$ is the dimensionless lower cutoff of scaling behavior (1)]. It is worth noticing that Eq. (94) converts into Eq. (86) if the fractal continuum flow obeys the Mandelbrot's rule of thumb (7). Furthermore, if $d_r = D-1$, but $n = d_\ell$ is fractional, Eq. (94) converts in the Barker Eq. (87) with $D^* = d_\ell$. Hence, physically, $D^*$ in Eq. (87) can be interpreted as the chemical dimension (23) of the radial fractal flow in a porous medium (see Fig. 3). This illustrates the difference between two fractal metrics, associated with the fractional Laplacian (16), (17) and the Hausdorff Laplacian (21), respectively.

In fact, Eqs. (87) and (94) describe two different pictures of fractal flow. Namely, Eq. (87) is associated with the flow field of the fractional topological dimension (see Fig. 3), but having the Euclidean metric (${}_{D^*}{}^{3}\Phi^{3}_{3} \subset E^3$), whereas Eq. (94) is associated with the fractal continuum flow ${}^{D}_{n}\Phi^{3}_{D} \subset E^3$. Phenomenologically, these equations can be combined by the replacing $n$ in Eq. (94) with the fractional chemical dimension $d_\ell$. Mathematically, this can be treated as the mapping of fractal flow in a porous medium ${}_{d_\ell}\Phi^{D}$ into the fractal continuum flow ${}^{D}_{d_\ell}\Phi^{3}_{D} \subset E^3$ by making use of the generalized fractional Laplacian (24) for the generalized fractal continuum flow ${}^{D}_{d_\ell}\Phi^{3}_{D} \subset E^3$. Physically, this mapping can be associated with a specific (although unknown) form of constitutive equation for the generalized fractal continuum flow ${}^{D}_{d_\ell}\Phi^{3}_{D} \subset E^3$. Although this statement is merely speculative, it has the same phenomenological basis as the introduction of the fractional Laplacian (16) in Refs. [26,27] and makes it possible to obtain the phenomenological pressure-transient equation (87) as a special case of the generalized pressure-transient Eq. (94), when equality (7) holds, while the flow dimension $n = d_\ell < 3$ is fractional. In the Cartesian coordinates the generalized pressure-transient equation for an anisotropic fractal continuum flow ${}^{D}_{d_\ell}\Phi^{3}_{D} \subset E^3$ has the following form:

$$\begin{aligned} c\mu_c\frac{\partial p}{\partial t} &= \sum_i^3 K^{(c)}_{ii}\left(\frac{x_i}{\ell_i}+1\right)^{2(1+d_i-D)}\left[\left(\frac{\partial^2(p-h_g)}{\partial x_i^2}\right)\right. \\ &\quad \left. + \frac{\alpha_i+d_i-D}{x_i+\ell_i}\left(\frac{\partial(p-h_g)}{\partial x_i}\right)\right], \end{aligned} \tag{96}$$

while the relationship (23) holds. In the case of $h_g = 0$ and $K^{(c)}_{ii} = K_0$ Eq. (96) can be rewritten in the following dimensionless form:

$$\frac{\partial p_D}{\partial t_D} = \Delta^H_D p,$$

where the generalized Laplacian is defined by Eq. (24) with dimensionless coordinates defined in Table IV. In the case of an isotropic fractal continuum flow ${}^{D}_{d_\ell}\Phi^{3}_{D} \subset E^3$, Eq. (96) can

TABLE V. Expressions for parameters of pressure-transient equations for radial flow in an isotropic fractally permeable reservoir expressed in the form of Eq. (98) and its analytical solution (100) with the initial and boundary conditions (99) corresponding to well production with a constant rate $Q = \text{const}$ for different pressure-transient models.

| Model and pressure-transient equation | $\gamma$ | $\beta$ | $\delta = 1 + \beta/\gamma$ |
|---|---|---|---|
| Euclidean, Eq. (86) | 2 | $n-2$ | $\frac{n}{2}$ |
| Barker, Eq. (87) | 2 | $D^*-2$ | $\frac{D^*}{2}$ |
| Chang and Yortsos, Eq. (89) | $2+\theta$ | $D_n-2-\theta$ | $\frac{D_n}{2+\theta}$ |
| ${}^{D}_{3}\Phi^{3}_{D}$, Eq. (94) | $2(D-d_r)$ | $n-1-D+d_r$ | $\frac{D-d_r-1+n}{2(D-d_r)}$ |
| ${}^{D}_{d_\ell}\Phi^{3}_{D}$, Eq. (97) | $2(D-d_r)$ | $d_\ell-1-D+d_r$ | $\frac{D-d_r-1+d_\ell}{2(D-d_r)}$ |

be rewritten in the following dimensionless form:

$$\frac{\partial p_D}{\partial t_D} = \left(\frac{r_D}{\ell_D}+1\right)^{d_r+2-D-d_\ell} \frac{\partial}{\partial r_D}\left[\left(\frac{r_D}{\ell_D}+1\right)^{d_r-D+d_\ell} \frac{\partial}{\partial r_D} p_D\right] = \left(\frac{r_D}{\ell_D}+1\right)^{2(d_r+1-D)} \left(\frac{\partial^2 p_D}{\partial r_D^2} + \frac{d_r+d_\ell-D}{r_D+\ell_D}\frac{\partial p_D}{\partial r_D}\right), \tag{97}$$

where the chemical dimension of fractal continuum flow ($d_\ell$) is determined by the fractional flow dimension ($\alpha$) of the fluid flow in a fractally permeable medium (see Fig. 3).

Regardless of the different physical contents, mathematically, the pressure-transient equations (86), (87), (89), (94), and (97) can be presented in the general dimensionless form as

$$r_D^{\gamma+\beta-1}\frac{\partial p_D}{\partial t_D} = \frac{\partial}{\partial r_D}\left(r_D^{\beta+1}\frac{\partial p_D}{\partial r_D}\right), \tag{98}$$

where the dimensionless variables and the scaling exponents $\beta$ and $\gamma$ for each pressure-transient equation are defined in Tables IV and V, respectively. Notice that Eq. (98) has the form of the equation for the radial diffusion on fractals suggested and analyzed in Refs. [56]. The authors of [56] have derived an exact analytical solution of this equation for radial diffusion from a point source. The radial pressure-transient equation of the type (98) was analyzed in the context of well tests in Refs. [6,57,62,63]. In a special case of well production with a constant rate $Q = \text{const}$ from an infinite reservoir the initial and boundary conditions are

$$p_D(r_D, t=0) = 0, \quad \lim_{r_D\to\infty} p_D(r_D, t_D) = 0,$$
$$\lim_{r_D\to 1} r_D^{\beta+1}\frac{\partial p_D}{\partial r_D} = -1, \tag{99}$$

where dimensionless parameters for different models are defined in Tables IV and V. An analytical solution of Eq. (98) with the initial and boundary conditions given by Eq. (99) can be presented in the following form:

$$p_D = \frac{x_D^{-\beta}}{\gamma\Gamma(\delta)}\Gamma\left(\delta-1, \frac{x_D^{\gamma}}{\gamma^2 t_D}\right), \tag{100}$$

where $\Gamma(a,y) = \int_x^\infty z^{a-1}e^{-z}dz$ is the incomplete $\Gamma$ function (see Refs. [57,62]). Notice that a few more analytical solutions of Eq. (98) have been suggested for some different sets of the initial and boundary conditions (see Refs. [6,57,63]).

Typical forms of pressure-transient behavior (100) are shown in Figs. 4–6. It is pertinent to note that these forms of pressure-transient curves are commonly observed in field drawdown tests (see, for review, Refs. [6,46,62,64–69]). It is worth noticing that if $d_\ell - 1 < D - d_r$, the pressure drop

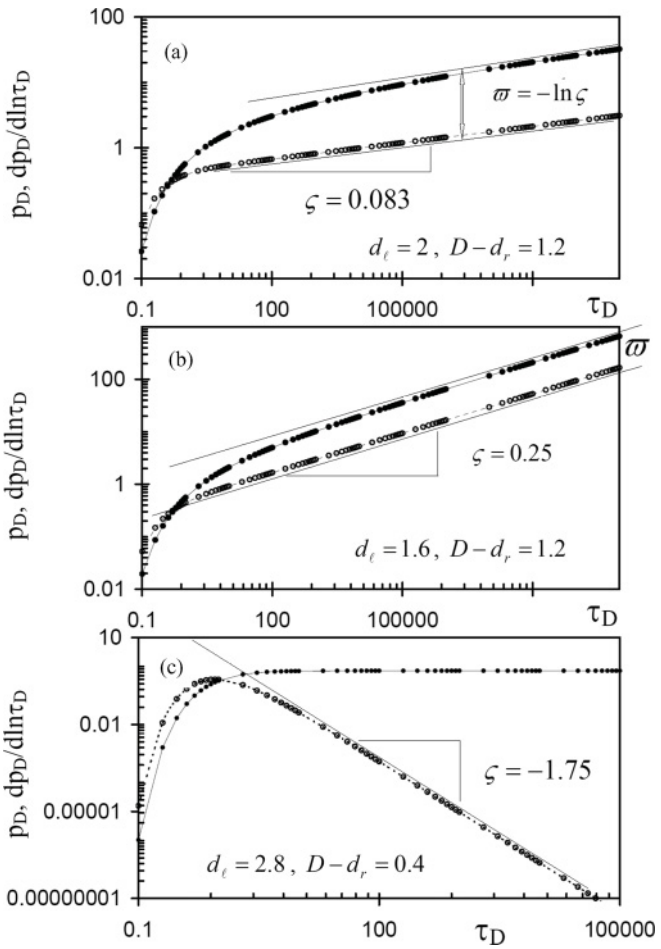


FIG. 4. Log-log plots of the dimensionless bottom hole pressure drops $p_D$ (solid circles) defined in Table IV and their derivatives $dp_D/d\ln\tau_D$ (open circles) versus the dimensionless time $\tau_D$ defined in Table IV from the numerical solution of Eq. (97) with scaling exponents defined in Table V for the cases of: (a) $d_\ell = 2$, $D - d_r = 1.2$; (b) $d_\ell = 1.6$, $D - d_r = 1.2$; and (c) $d_\ell = 2.8$, $D - d_r = 0.4$. Curves, data fitting with Eq. (100); straight lines are guides for the eye showing the power-law behavior with the scaling exponent $\varsigma$.

and its logarithmic derivative both obey the same power-law asymptotic behavior $p_D \propto \partial p_D/\partial \ln t_D \propto t_D^{\varsigma}$ [see Figs. 4(a), 4(b), and 5], with the scaling exponent

$$\varsigma = \frac{1}{2} + \frac{1-d_\ell}{2(D-d_r)}, \tag{101}$$

such that two log-log graphs are offset at $\ln t_D = 0$ by the constant $\varpi = -\ln \varsigma$ [see Figs. 4(a) and 4(b)]. Such behavior was observed in many real field experiments and is commonly used for fast estimation of aquifer fractal properties (see, for example, Refs. [64–69]). In the opposite case of $d_\ell - 1 > D - d_r$ the derivative of $p_D$ with respect to $\ln t_D$ displays the asymptotic power-law behavior with $\varsigma < 0$ [see Fig. 4(c) and curve (8) in Fig. 5(b)], but the pressure behavior does not have a power-law asymptotic [see Fig. 4(c) and curve (8) in Fig. 5(a)].

It is pertinent to point out that the pressure drop is localized in the well vicinity region, the size of which, defined as $R_D = r_D(p_D = 10^{-5} \ll 1, t)$ [see Figs. 6 and 7(a)], increases in time as $R_D \propto t^{1/\gamma}$ (see Fig. 7 and Table V). This scaling behavior, which was observed in the field experiments, has given a reason to talk about an anomalous diffusion in fractally permeable reservoirs (see Refs. [57,64]). In fact, however, an anomalous scaling of $R_D$ [presented in Fig. 7(b)] can be attributed to the fractional topology (see Fig. 3) of the Darcian

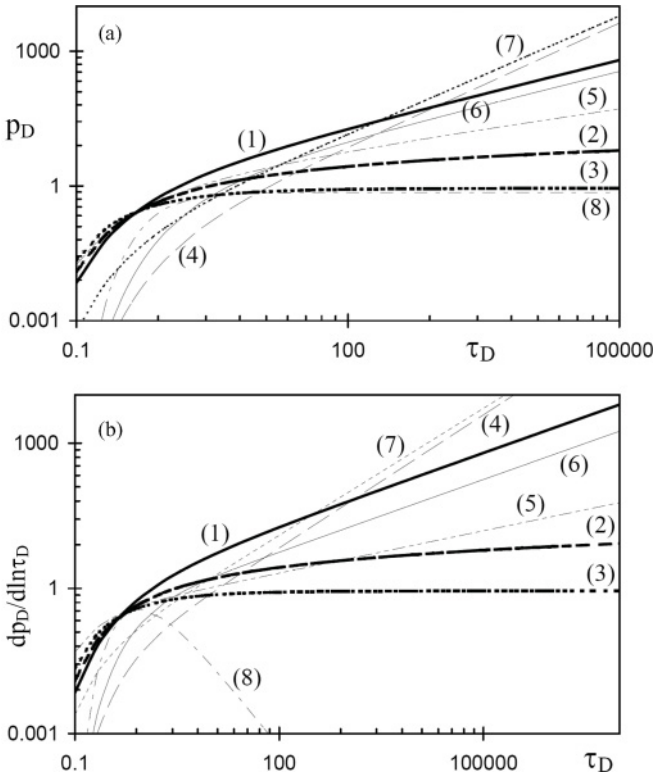


FIG. 5. Log-log plots of the dimensionless: (a) bottom hole pressure drops $p_D$ and (b) derivatives $dp_D/d\ln\tau_D$ versus the dimensionless time $\tau_D$ (defined in Table IV) calculated using Eq. (100) with the scaling exponents defined in Table V for Eq. (97) for the cases of $d_\ell = 1$ and $D - d_r = 1$ (1), $d_\ell = 2$ and $D - d_r = 1$ (2), $d_\ell = 3$ and $D - d_r = 1$ (3), $d_\ell = 0.5$ and $D - d_r = 0.6$ (4), $d_\ell = 1.5$ and $D - d_r = 1.2$ (5), $d_\ell = 1$ and $D - d_r = 0.5$ (6), $d_\ell = 0.25$ and $D - d_r = 1$ (7), and $d_\ell = 2.8$ and $D - d_r = 0.4$ (8).

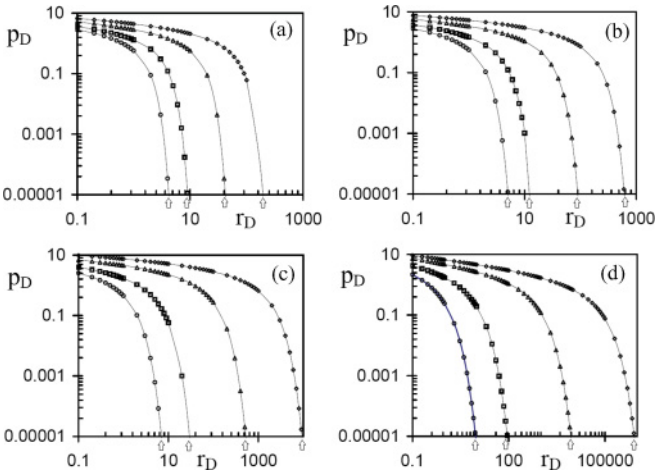


FIG. 6. Log-log plots of dimensionless pressure drops $p_D$ versus dimensionless distance from well $r_D$ for different dimensionless times $t_D$ =1 (circles), $t_D$ =10 (squares), $t_D$ =1000 (triangles), and $t_D$ = 100 000 (diamonds) from the numerical solution of Eq. (97) with scaling exponents defined in Table V for the cases of fractal continuum flow with: (a) $d_\ell = 2.5$ and $D - d_r = 1.5$, (b) $d_\ell = 2.2$ and $D - d_r = 1.2$, (c) $d_\ell = 1.8$ and $D - d_r = 0.8$, (d) $d_\ell = 1.6$ and $D - d_r = 0.5$. Curves, data fitting with Eq. (100); arrows indicate the dimensionless size of transient zone $R_D = r_D(p_D = 10^{-5}, t)$.

fractal continuum flow ${}^{D}_{d_\ell}\Phi^3_D \subset E^3$, rather than to an anomalous diffusion (see Tables II and V).

Here, it should be emphasized that the Euclidean (86) and Barker (87) models can be treated as special cases of the fractal continuum flow model (97) (see Table V and Fig. 5). Furthermore, regardless of the fundamental difference of physical models leading to the pressure-transient equations (89) and (97), these equations are mathematically equivalent. Therefore, both equations have identical numerical solutions

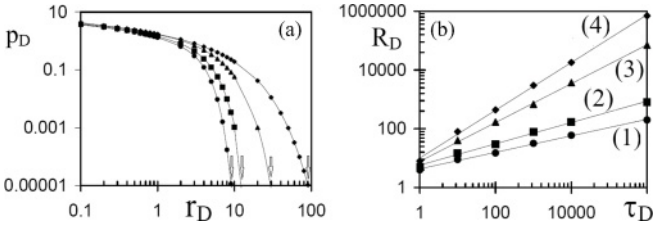


FIG. 7. (a) Log-log plots of dimensionless pressure drops $p_D$ versus dimensionless distance from well $r_D$ (defined in Table IV) from the numerical solution of Eq. (97) with scaling exponents defined in Table V for time $t_D$ =10 in the cases of fractal continuum flow with $d_\ell = 2.5$ and $D - d_r = 1.5$ (solid circles), $d_\ell = 2.2$ and $D - d_r = 1.2$ (solid squares), $d_\ell = 1.8$ and $D - d_r = 0.8$ (solid triangles), $d_\ell = 1.6$ and $D - d_r = 0.5$ (solid diamonds); curves, data fitting with Eq. (100); arrows indicate the dimensionless size of transient zone $R_D$. (b) Log-log plots of dimensionless size of transient zone $R_D$ versus dimensionless time $t_D$ from the numerical solution of Eq. (98) with scaling exponents defined in Table V for the fractal continuum flow with $d_\ell = 2.5$ and $D - d_r = 1.5$ (solid circles), $d_\ell = 2.2$ and $D - d_r = 1.2$ (solid squares), $d_\ell = 1.8$ and $D - d_r = 0.8$ (solid triangles), $d_\ell = 1.6$ and $D - d_r = 0.5$ (solid diamonds); straight lines, data fittings with the power law $R_D \propto t^{1/\gamma}$ with $\gamma$ =3 (1), 2.4 (2), 1.6 (3), and 1 (4).

TABLE VI. Results of the field data fitting with Eqs. (89) and (97). Experimental field data and fitting parameters of Eq. (89) are taken from Refs. [65–68], while the fitting parameters of Eq. (97) are calculated using relationships (102) and (103).

| | Eq. (89) | | Eq. (97) | |
|---|---|---|---|---|
| Field, Well | $D_n$ | $\theta$ | $D-d_r$ | $d_\ell$ |
| Kamonjang field data [65] | 1.6 | 0.5 | 1.25 | 1.35 |
| Kizildere field data [66] | 1.66 | 0.5 | 1.25 | 1.41 |
| Aquifer in Poitiers, Well M1 [67] | 3.57 | 3.36 | 2.68 | 1.89 |
| Aquifer in Poitiers, Well M5 [67] | 2.83 | 2.25 | 2.125 | 1.705 |
| Aquifer in Plomeur, Well R46 [68] | 2.49 | 1.73 | 1.865 | 1.625 |
| Aquifer in Plomeur, Well R61 [68] | 3.26 | 2.89 | 2.445 | 1.815 |
| Aquifer in Plomeur, Well R200 [68] | 2.54 | 1.81 | 1.905 | 1.635 |
| Aquifer in Plomeur, Well R200b [68] | 1.48 | 0.23 | 1.115 | 1.365 |
| Aquifer in Plomeur, Well R273 [68] | 1.91 | 0.82 | 1.41 | 1.5 |
| Aquifer in Plomeur, Well R385 [68] | 1.81 | 0.72 | 1.36 | 1.45 |

in the dimensionless variables when

$$\theta = 2(D - d_r - 1), \tag{102}$$

while

$$D_n = d_\ell + (D - d_r - 1) = d_\ell + \theta/2, \tag{103}$$

and so the corresponding spectral dimension of the flow modeled by Eq. (89) is equal to

$$d_s^n = 1 + \frac{d_\ell - 1}{D - d_r}, \tag{104}$$

whereas the spectral dimension of fractal continuum is equal to its mass fractal dimension, that is, $d_s = D$ (see Table II). It should be emphasized that equalities (102)–(104) are of pure numerical nature and have no physical meaning. Even so, this observation has very important practical implications. In fact, although the physical basis of Eq. (89) is at least questionable (e.g., see the discussion about anomalous diffusion in Secs. III C and III D), it is widely used in the petroleum engineering also. In this context, the successful applications of Eq. (89) to fit the experimental pressure-transient data have been reported by several authors (see, for example, Refs. [6,64–68] and references therein). However, it should be pointed out that in all applications the exponents $D_n$ and $\theta$ were used as fitting parameters, but were not estimated from experiments. On the other hand, relationships (102) and (103) make it possible to fit the same experimental data using Eq. (97) based on the fractal continuum hydrodynamics (e.g., see Table VI). Furthermore, the general pressure-transient equation (96) with appropriate boundary and initial conditions can be used for numerical simulations of three-dimensional flows in anisotropic fractally permeable reservoirs, whereas the generalization of Eq. (89) for anisotropic reservoirs is not a straightforward matter. Moreover, in contrast to the anomalous diffusion exponent used as the fitting parameter only, the scaling parameters of Eqs. (96) and (97) can be obtained from independent field experiments on the reservoir fractal characterization (e.g., see Refs. [69]).

## V. CONCLUSIONS

Summarizing, in this work the hydrodynamics of fractal continuum flow ${}^{D}_{3}\Phi^3_D \subset E^3$ is developed on the basis of self-consistent model of fractal continuum. Besides, a phenomenological generalization of the pressure-transient equation for generalized fractal continuum flow ${}^{D}_{d_\ell}\Phi^3_D \subset E^3$ is suggested. It is shown that the classical pressure-transient equations for the flow in fractally permeable media can be obtained as the special cases of the generalized pressure-transient equation for fractal continuum flow. In this context, the celebrated Barker's equation was generalized for an anisotropic fractional flow in the three-dimensional reservoirs. It is shown that the pressure-transient equation based on the fractal continuum hydrodynamics provides a good fitting of the field experimental data reported in the literature.

It is pertinent to note that the fractal continuum hydrodynamics developed in this work can be easily generalized for the case of multiphase flow. The double [45,57] and triple [70] porosities of many real aquifers can be accounted for by the consideration of two or three coupled continuum flows. Furthermore, the finite aquifer size and the well damage can be easy accounted for by the modification of boundary conditions, as is suggested in Refs. [57,71]. In this context, Eq. (96) with appropriate boundary and initial conditions can be used for numerical simulations of different pressure-transient tests (drawdown, buildup, injection, fallow, and interference) in anisotropic fractally permeable reservoirs. In these simulations the fractal dimensions $D$, $d_i$, and $d_\ell$ can be either used as the fitting parameters to fit the experimental field data, or independently determined from the fractal analysis of the reservoir.

The results reported in this paper provide an insight into the hydrodynamics of fluid flow in fractally permeable media and can be used to improve the fractal approach to model the pumping well pressure response that is widely used in petroleum engineering. Moreover, the fractal continuum flow approach leads to a radical change of paradigm in the well test interpretation. In fact, the pressure response of fractal continuum flow is governed by the fractional topology and metric of fractally permeably medium, rather than by an anomalous diffusion. Besides, the fractal continuum framework developed in this work can be employed to model other problems arising in the mechanics of fractal media.

**ACKNOWLEDGMENTS**

The authors thank Rodolfo Camacho-Velázquez from the Mexican Petroleum Company (PEMEX), Yannis C. Yortsos (University of Southern California), Armando García Jaramillo (TEMPLE), and Carlos Lira-Galeana (Mexican Petroleum Institute) for fruitful and clarifying discussions. This work was partially supported by the PEMEX under the research SENER-CONACYT Grants No. 143927 and No. 116458.

[1] J. Bear, *The Dynamics of Fluids in Porous Media* (Dover, Mineola, NY, 1988); M. Sahimi, *Flow and Transport in Porous Media and Fractured Rock* (VCH, Weinheim, 1995); M. Sahimi in *Flow and Transport in Fractured Porous Media*, edited by P. Dietrich *et al*. (Springer, Berlin, 2005).

[2] A. J. Katz and A. H. Thompson, Phys. Rev. Lett. **54**, 1325 (1985); A. P. Radlinski, E. Z. Radlinska, M. Agamalian, G. D. Wignall, P. Lindner, and O. G. Randl, *ibid*. **82**, 3078 (1999); K. Oleschko, G. Korvin, A. S. Balankin, R. V. Khachaturov, L. Flores, B. Figueroa, J. Urrutia, and F. Brambila, *ibid*. **89**, 188501 (2002); K. Oleschko, G. Korvin, B. Figueroa, M. A. Vuelvas, A. S. Balankin, L. Flores, and D. Carreón, Phys. Rev. E **67**, 041403 (2003).

[3] A. S. Balankin, T. López, R. Alexander-Katz, A. Córdova, O. Susarrey, and R. Montiel, Langmuir **19**, 3628 (2003); T. López, F. Rojas, R. Alexander-Katz, F. Galindo, A. S. Balankin, and A. Buljan, J. Solid State Chem. **177**, 1873 (2004); T. López, M. Patiño-Ortiz, A. S. Balankin, and R. D. González, Appl. Mech. Mat. **15**, 121 (2009); Y. Ono, H. Mayama, I. Furó, A. I. Sagidullin, K. Matsushima, H. Ura, T. Uchiyama, and K. Tsujii, J. Colloid Interface Sci. **336**, 215 (2009).

[4] D. Giménez, E. Perfect, W. J. Rawls, and Y. Pachepsky, Eng. Geol. **48**, 161 (1997); K. Oleschko, Soil Tillage Res. **49**, 255 (1998); A. Dathea and M. Thullner, Geoderma **129**, 279 (2005); K. Oleschko, G. Korvin, L. Flores, F. Brambila, C. Gaona, J. F. Parrot, G. Ronquillo, and S. Zamora, *ibid*. **160**, 93 (2010); Y. Zaretskiy, S. Geiger, K. Sorbie, and M. Förster, Adv. Water Res. **33**, 1508 (2010); A. Ahmadi, M. R. Neyshabouri, H. Rouhipour, and H. Asadi, J. Hydrol. **400**, 305 (2011); H. Dashtian, G. R. Jafari, M. Sahimi, and M. Masihi, Physica A **390**, 2096 (2011).

[5] J. Fuite, R. Marsh, and J. Tuszynski, Phys. Rev. E **66**, 021904 (2002); S. W. Coleman and J. C. Vassilicos, Phys. Rev. Lett. **100**, 035504 (2008); A. M. Tartakovsky, D. M. Tartakovsky, and P. Meakin, *ibid*. **101**, 044502 (2008); P. S. Kondratenko and L. V. Matveev, Phys. Rev. E **83**, 021106 (2011).

[6] F. J. Fayers and T. A. Hewett, Adv. Water Res. **15**, 341 (1992); H. Jourde, S. Pistre, P. Perrochet, and C. Drogue, *ibid*. **25**, 371 (2002); L. Guarracino and J. E. Santos, Math. Geol. **36**, 217 (2004); P. Xu, B. Yu, S. Qiu, and J. Cai, Physica A **387**, 6471 (2008); K. C. Hsu and K. C. Chen, Stoch. Environ. Res. Risk Assess. **24**, 1053 (2010); S. A. Fomin, V. A. Chugunov, and T. Hashida, Adv. Water Res. **34**, 205 (2011); V. R. Voller, *ibid*. **34**, 257 (2011).

[7] A. S. Balankin, O. Susarrey, and J. Márquez, Phys. Rev. Lett. **90**, 096101 (2003); A. S. Balankin, R. García, O. Susarrey, D. Morales, and F. Castrejon, *ibid*. **96**, 056101 (2006); A. S. Balankin, S. Matías, D. Samayoa, J. Patiño-Ortiz, B. Espinoza, and C. L. Martínez, Phys. Rev. E **83**, 036310 (2011).

[8] A. S. Balankin and B. Espinoza, Phys. Rev. E **85**, 025302(R) (2012).

[9] M. Schmutz, Europhys. Lett. **2**, 897 (1986).

[10] M. Porto, A. Bunde, S. Havlin, and H. E. Roman, Phys. Rev. E **56**, 1667 (1997).

[11] S. Havlin and D. Ben-Avraham, Adv. Phys. **36**, 695 (1987); **51**, 187 (2002).

[12] A. V. Milovanov, Phys. Rev. E **56**, 2437 (1997).

[13] G. Calcagni, Phys. Rev. Lett. **104**, 251301 (2010); S. I. Muslih and O. P. Agrawal, J. Math. Phys. **50**, 123501 (2009).

[14] U. Mosco, Phys. Rev. Lett. **79**, 4067 (1997).

[15] T. Nakayama, K. Yakubo, and R. L. Orbach, Rev. Mod. Phys. **66**, 381 (1994).

[16] K. Falconer, *Fractal Geometry—Mathematical Foundations and Applications* (Wiley, New York, 1990).

[17] J. Feder, *Fractals* (Plenum, New York, 1988).

[18] F. M. Borodich and Z. Feng, Z. Angew. Math. Phys. **61**, 21 (2010).

[19] H. E. Stanley and A. Coniglio, Phys. Rev. B **29**, 522 (1984).

[20] I. I. Bogdanov, V. V. Mourzenko, and J.-F. Thovert, Phys. Rev. E **76**, 036309 (2007); P. A. Cello, D. D. Walker, A. J. Valocchi, and B. Loftis, Vadose Zone J. **8**, 258 (2009).

[21] V. V. Mourzenko, J.-F. Thovert, and P. M. Adler, Phys. Rev. E **59**, 4265 (1999); G. Drazer and J. Koplik, *ibid*. **62**, 8076 (2000); G. Gioia1 and F. A. Bombardelli, Phys. Rev. Lett. **88**, 014501 (2002); J. S. Andrade, A. D. Araujo, M. Filoche, and B. Sapoval, *ibid*. **98**, 194101 (2007); A. Cortisa and J. G. Berryman, Phys. Fluids **22**, 053603 (2010); L. Talon, H. Auradou, and A. Hansen, Phys. Rev. E **82**, 046108 (2010).

[22] S. Miyazima and H. E. Stanley, Phys. Rev. B **35**, 8898 (1987).

[23] V. E. Tarasov, *Fractional Dynamics* (Springer, New York, 2010).

[24] J.-P. Bouchaud and A. Georges, Phys. Rep. **195**, 127 (1990); A. Compte and R. Metzler, J. Phys. A: Math. Gen. **30**, 7277 (1997); R. Metzler and J. Klafter, Phys. Rep. **339**, 1 (2000); V. V. Uchaikin, Phys. Usp. **46**, 821 (2003); L. M. Zeleni and A. V. Milovanov, *ibid*. **47**, 749 (2004); V. E. Tarasov, Ann. Phys. **323**, 2756 (2008); E. Baskin and A. Iomin, Chaos Solitons Fractals **44**, 335 (2011).

[25] K. M. Kolwankar and A. D. Gangal, Chaos **6**, 505 (1996); A. Babakhani and V. Daftardar-Gejji, J. Math. Anal. Appl. **270**, 66 (2002); A. Carpinteri, P. Cornetti, A. Sapora, M. Di Paola, and M. Zingales, Phys. Scr., T **136**, 014003 (2009); Y. Chen, Y. Yan, and K. Zhang, J. Math. Anal. Appl. **362**, 17 (2010).

[26] F. H. Stillinger, J. Math. Phys. **18**, 1224 (1977).

[27] C. Palmer and P. N. Stavrinou, J. Phys. A **37**, 6987 (2004).

[28] W. Chen, Chaos, Solitons Fractals **28**, 923 (2006).

[29] V. E. Tarasov, Adv. Ann. Phys. **318**, 286 (2005).

[30] V. E. Tarasov, Phys. Plasmas **13**, 052107 (2006).

[31] Notice that in Refs. [29,30] the fractional divergence is introduced in the form obeying the postulated form of the Green-Gauss theorem for the proposed model of fractal continuum and

then (in appendixes) the generalized forms of Green-Gauss an Kelvin-Stokes theorems are derived using the suggested forms of fractional differential vector operators.

[32] J. Harrison, Bull. Am. Math. Soc. **29**, 235 (1993).

[33] J. Harrison and A. Norton, Duke J. Math. **67**, 575 (1992); J. Harrison, J. Phys. A: Math. Gen. **32**, 5317 (1999); F. M. Borodich and A. Yu. Volovikov, Proc. R. Soc. London A **456**, 1 (2000); T. J. Lyons and P. S. C. Yam, J. Math. Pures Appl. **85**, 38 (2006); J. Huikun and G. Zheng, J. Math. Anal. Appl. **355**, 164 (2009).

[34] V. E. Tarasov, Phys. Plasm. **12**, 082106 (2005); M. M. Meerschaert, J. Mortensen, and S. W. Wheatcraft, Physica A **367**, 181 (2006); A. N. Bogolyubov, A. A. Potapov, and S. S. Rehviashvili, Moscow Univ. Phys. Bull. **64**, 365 (2009); R. Almeida, A. B. Malinowska, and D. F. M. Torres, J. Math. Phys. **51**, 033503 (2010); E. Baskin and A. Iomin, Chaos Solitons Fractals **44**, 335 (2011).

[35] J. Li and M. Ostoja-Starzewski, Proc. Royal Soc. A (London) **465**, 2521 (2009); Formamente **4**, 93 (2011); P. N. Demmie and M. Ostoja-Starzewski, J. Elasticity **104**, 187 (2011).

[36] G. F. Pinder and W. G. Gray, *Essentials of Multiphase Flow and Transport in Porous Media* (Wiley, New Jersey, 2008).

[37] L. D. Landau and E. M. Lifshitz, *Fluid Mechanics*, 2nd English edition (Pergamon, Oxford, 1987).

[38] Although Navier-Stokes equations were written down in the 19th century, no proof has yet been found guaranteeing even the existence of a smooth solution in just three dimensions. This is known as the Navier-Stokes existence and smoothness problem. For its solution the Clay Mathematics Institute offered a US $1,000,000 prize, which has yet to be claimed.

[39] S. Whitaker, *The Method of Volume Averaging* (Kluwer Academic, Netherlands, 1999).

[40] D. M. Tartakovskya, Z. Lub, A. Guadagninic, and A. M. Tartakovsky, J. Hydrology **275**, 182 (2003).

[41] S. Alexander and R. Orbach, J. Phys. (Paris), Lett. **43**, L625 (1982).

[42] A. Telcs, Probab. Theory Relat. Fields **82**, 435 (1989).

[43] A. Telcs, J. Theor. Probab. **8**, 77 (1995).

[44] C. P. Haynes and A. P. Roberts, Phys. Rev. Lett. **103**, 020601 (2009).

[45] H. Cinco-Ley and F. Samaniego, J. Pet. Technol. **33**, 1749 (1981).

[46] T. Ahmed and P. D. McKinney, *Advanced Reservoir Engineering* (Elsevier, New York, 1989); R. N. Horne, *Modern Well Test Analysis: A Computer-Aided Approach* (Petroway, Inc., Palo Alto, CA, 1990); Zh. Chen, G. Huan, and Y. Ma, *Computational Methods for Multiphase Flows in Porous Media* (SIAM, Philadelphia, 2006).

[47] M. R. Madhav and P. Basak, J. Hydrology **34**, 21 (1977); S. M. Hassanizadeh, and W. G. Gray, Transp. Porous Med. **2**, 521 (1987); D. A. Edwards, M. Shapiro, P. Bar-Yoseph, and M. Shapira, Phys. Fluids **2**, 45 (1990); D. Ruth and H. Ma, Transp. Porous Med. **7**, 255 (1992); T. Kohl, K. F. Evans, R. J. Hopkirk, R. Jung, and L. Rybach, Water Res. Res. **33**, 407 (1997); I. S. Bennethum, M. A. Murad, and J. H. Cushman, Comp. Geotechn. **20**, 245 (1997); R. J. Hill, D. L. Koch, and A. J. C. Ladd, J. Fluid Mech. **448**, 213 (2001); R. J. Hill and D. L. Koch, *ibid*. **465**, 59 (2002); K. N. Moutsopoulos, I. N. E. Papaspyros, and V. A. Tsihrintzis, J. Hydrology **374**, 242 (2009); Y. Yuedong and G. Jiali, Pet. Sci. **8**, 55 (2011); J. Niessner, S. Berg, and S. M. Hassanizadeh, Transp. Porous Med. **88**, 133 (2011).

[48] M. K. Hubbert, J. Geology **48**, 785 (1940).

[49] S. M. Hassanizadeh and W. G. Gray, Adv. Water Resour. **3**, 25 (1980).

[50] S. Whitaker, Ind. Eng. Chem. **61**, 14 (1969); J. Barrere, G. Olivier, and S. Whitaker, Trans. Porous Media **7**, 209 (1992).

[51] X. Du and M. Ostoja-Starzewski, Proc. R. Soc. A **462**, 2949 (2006); E. G. Shifrin and N. A. Gusev, Doklady Physics **55**, 615 (2010); J. Niessner, S. Berg, and S. M. Hassanizadeh, Transp. Porous Med. **88**, 133 (2011).

[52] A. Le Mehaute and G. Crepy, Solid State Ionics **9-10**, 17 (1983); A. Le Mehaute, J. Stat. Phys. **36**, 665 (1984); R. R. Nigmatullin, Phys. Status Solidi B **133**, 425 (1986); V. N. Belonenko, O. Y. Dinariev, and A. B. Mosolov, Sov. Phys. Solid State Phys. **56**, 83 (1986); A. Compte and D. Jou, J. Phys. A: Math. Gen. **29**, 4321 (1996).

[53] H. Ji-Huan, J. Comput. Methods Appl. Mech. Eng. **167**, 57 (1998).

[54] M. Caputo, Water Res. Research **36**, 693 (2000).

[55] G. van Tonder, K. Riemann, and I. Dennis, Hydrogeol. J. **10**, 351 (2002); K. Riemann, G. van Tonder, and P. Dzanga, *ibid.* **10**, 357 (2002).

[56] B. O'Shaugnessy and I. Procaccia, Phys. Rev. Lett. **54**, 455 (1985); Phys. Rev. A **32**, 3073 (1985).

[57] J. Chang and Y. C. Yortsos, SPE Form. Eval. **5**, 31 (1990).

[58] A. Cloot and J. F. Botha, Water SA **32**, 1 (2006); M. Khan, T. Hayat, and S. Asghar, Int. J. Eng. Sci. **44**, 333 (2006).

[59] J. A. Ochoa, F. J. Valdes, and J. Alvarez, Physica A **374**, 1 (2007).

[60] S. Whitaker, Transp. Porous Media **1**, 3 (1986).

[61] W. F. Brace, J. Geophy. Res. **89**, 4327 (1984); H. Schad and G. Teutsch, J. Hydrol. **159**, 61 (1994); C. W. Rovey and D. S. Cherkauer, Ground Water **33**, 769 (1995); D. Schulze-Makuch, D. A. Carlson, D. S. Cherkauer, and P. Malik, *ibid*. **37**, 904 (1999); A. G. Hunt, Hydrogeology J. **14**, 499 (2006).

[62] J. A. Barker, Water Res. Res. **24**, 1796 (1988).

[63] L. M. Bangoy and C. Drogue, J. Hydrolog. **158**, 47 (1994); H. W. Park, J. Choe, and J. M. Kang, Energy Sources **22**, 881 (2000); H. W. Park, J. Choe, and J. M. Kang, *ibid*. **23**, 619 (2001).

[64] J. A. Acuna and Y. C. Yortsos, Water Res. Res. **31**, 527 (1995); F. Flamenco-López and R. Camacho-Velazques, SPE Res. Eval. Eng. **6**, 39 (2003); R. Camacho-Velázquez, G. Fuentes-Cruz, and M. Vasquez-Cruz, *ibid.* **11**, 606 (2008); R. Raghavan, J Petroleum Sci. Eng. **80**, 7 (2011).

[65] S. Aprllian, D. Abdassah, L. Mucharam, and R. Sumantri, SPE **26465**, 511 (1993).

[66] M. Onur, A. D. Zeybek, U. Serpen, and I. M. Gok, Geothermics **32**, 147 (2003).

[67] S. Bernard, F. Delay, and G. Porel, J. Hydrol. **328**, 647 (2006).

[68] T. Le Borgne, J. R. de Dreucy, P. Davy, and F. Touchard, Water Resour. Res. **40**, W03512 (2006).

[69] H. Dong and M. J. Blunt, Phys. Rev. E **80**, 036307 (2009); J. Liu and K. Regenauer-Lieb, *ibid.* **83**, 016106 (2011).

[70] D. Abdassah and I. Ershaghi, SPE Form. Eval. **1** 113 (1986).

[71] Y. Zhao and L. Zhang, World J. Mech. **1**, 209 (2011).